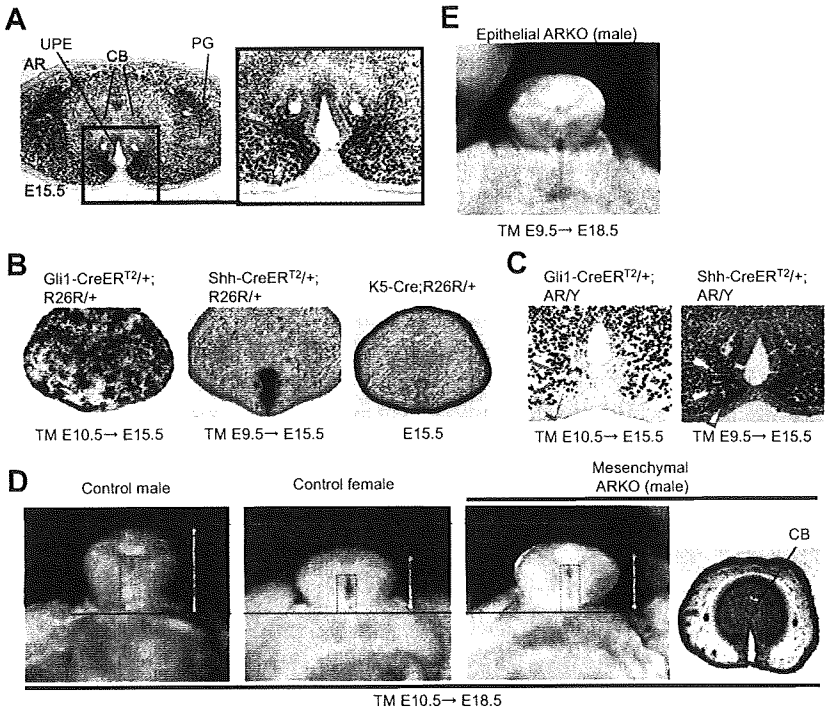

FIG. 2. Involvement of the mesenchymally expressed AR for external genital masculinization. A, AR is expressed in both the UPE and the mesenchyme of the male GT at E15.5. Note the prominent expression in the mesenchyme adjacent to the UPE in the male GTs (*arrowheads*). CB, Prospective corporal body; PG, preputial gland. B, Targeted recombination driven by Gli1^{CreERT2}, Shh^{CreERT2}, and K5-Cre driver mice was assessed with Rosa26 reporter (R26R) mice. The TM was administrred at E10.5 or E9.5, respectively, and the labeled tissue was assessed at E15.5. The sections are counterstained with eosin. C, AR expression in the GTs of the mesenchyme- and epithelium-specific ARKO mice. In the mesenchymal KO mice, the mesenchymal AR expression is observed as a dispersed manner (*arrowheads*). D, The phenotypes of tissue-specific conditional ARKO mice. The mesenchyme-specific ARKO male mice exhibit hypoplastic external genitalia (*arrows*) with an unclosed prepuce similar to the control female GTs (*red boxes*). Histological sections also show the female-like GTs in the male mutants (compare that with Fig. 1A). E, The GTs of the epithelium-specific ARKO male mice appear morphologically indistinguishable from those of the control males.

to identify the candidate masculine effectors for embryonic organogenesis.

Results

Critical time window of androgen actions on GT masculinization

One of the characteristics of the development of the embryonic external genitalia, the GTs, is the prominent morphological sexual dimorphisms, which are already evident in the later stage of embryogenesis. This makes GTs ideal subjects to study the mechanisms of sexual development in mammals. Before elucidating the contribution of growth factor signaling in GT masculinization, it is necessary to clarify the spatially and temporally regulated androgen signaling. Therefore, this study initially attempted to define the critical time window for differentiation into the male sexual characteristics of the GTs.

To define the critical time window of androgen actions for GT masculinization, antiandrogenic chemical exposure experiments for mouse embryos were performed *in utero*. GT masculinization can be defined with morphological criteria, the formation of a tubular urethra with well-developed prepuce, and the condensation of a bilaterally segmented prospective corporal body (Fig. 1A). In contrast to such male characteristics, female GTs do not form a tubular urethra and exhibit an unclosed prepuce at the lower (ventral) midline of the GTs (*arrowheads* in Fig. 1A).

The intrauterine exposure of flutamide demasculinizes the external genitalia of male rodent offspring (14, 15, 27). To accurately examine the timing of GT masculinization, the modulation of the masculine processes was attempted by administering two successive injections of flutamide at various stages during pregnancy. The resultant morphologies of the embryonic GTs were then analyzed at E18.5 (see treatment timeline, Fig. 1B). The GTs of male mouse embryos treated with flutamide on E13.5–14.5 and E14.5–15.5 displayed normal male-type morphology (data not shown). In contrast, when the embryos were treated with flutamide on E15.5–16.5 and E16.5–17.5 (*red lines* in the timeline), the GTs were demasculinized and their morphologies were similar to those of the female GTs (Fig. 1B). In addition, female GTs were masculinized when the embryos were treated with testosterone propionate at E15.5–16.5 (Fig. 1B). Based on these observations, the critical time window of GT masculinization regulated by androgens is demonstrated as E15.5–16.5 in mice.

Spatially regulated androgen signals for masculinization processes of external genitalia

Epithelial-mesenchymal interactions between the UPE and its adjacent mesenchyme have been suggested to play an essential role during external genital formation. A tissue-recombination study suggested that the GT mesenchyme induces mature urethral epithelia formation (16). On the other hand, the UPE is thought to play an inductive role in mesenchymal differentiation (17, 28). However, the region-specific androgen function mediated by each epithelially and mesenchymally expressed AR, if any, has never been analyzed. In fact, the expression of AR has been found in both the UPE and mesenchyme at E15.5, the currently identified time window for masculinization (Fig. 2A). A region-specific conditional AR knockout (KO) mouse study was therefore conducted to analyze the mesenchymally or epithelially expressed AR functions in GTs; the mesenchymal tissue-specific KO of AR was first examined using Gli1^{CreERT2} mice (hereafter referred to as mesenchymal ARKO). Gli1 is expressed in the mesenchyme around the cloacal epithelium (pericloacal mesenchyme) at E10.5 (29). The cells from the pericloacal mesenchyme contribute to the external genital mesenchyme in the later stages (29). The mice were shown to be an effective

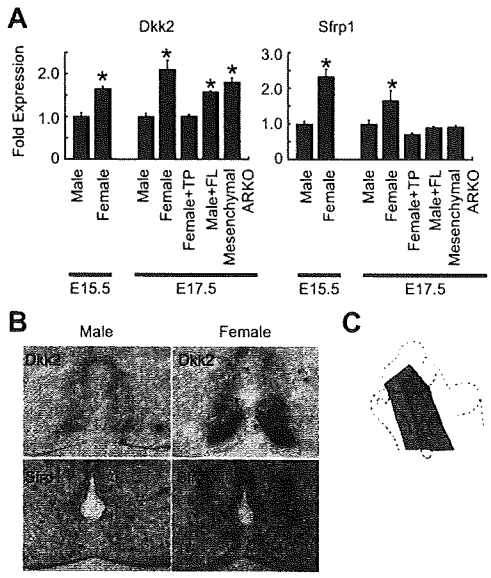

FIG. 3. Wnt/β-catenin signaling during GT development. A, A quantitative RT-PCR analysis reveals the expression of Dkk2 and Sfrp1 to increase in wild-type females in comparison with those of wild-type males at E15.5 and E17.5. Dkk2 expression is increased in the male GTs treated with flutamide (FL) and the GTs of mesenchymal ARKO mice. The tissue specimens are collected from the mesenchyme adjacent to the UPE of the GTs (*blue area* in C). TP, Testosterone propionate. *, $P < 0.05$ *vs.* control male. B, Dkk2 and Sfrp1 expression is abundantly detected in the wild-type female in comparison with those of the wild-type male at E15.5.

Cre line for targeted recombination in the urogenital organ mesenchyme [samples treated with tamoxifen (TM) at E10.5 are examined at E15.5; Fig. 2B]. AR is significantly expressed in the mesenchyme adjacent to the urethral epithelium (Fig. 2A). In fact, in the mesenchymal ARKO mice, the mesenchymal AR tends to be expressed in dispersed manner (*arrowhead* in Fig. 2C).

Mesenchymal ARKO mice exhibited hypoplastic external genitalia with an undeveloped prepuce, which are characteristics morphologically similar to the female GTs (six of six embryos; Fig. 2D). In the wild-type male GTs, a marked degree of bilaterally segmented mesenchymal condensations was notably observed in the developing male GTs at the late stage (Fig. 1A). However, the prospective corporal bodies, defined by the histological criteria as mesenchymal condensation, neither differentiated nor bilaterally segmented in the mesenchymal ARKO mice (Fig. 2D). On the other hand, the development of the internal reproductive organs of such mesenchymal ARKO mice was basically not affected in comparison with the development of the control male organs (data not shown).

To exclude the possibility of the phenotype elicited by a low level of Cre activity in the ectoderm of the Gli1^{CreERT2} line (Fig. 2B), the ectoderm-specific ARKO mice were also analyzed using a Cre-expressing line under a keratin 5 promoter (K5-Cre; Fig. 2B) (30). These mice did not display any defects in the GT masculinization (data not shown). This is consistent with the lack of AR expression in the GT ectoderm (Fig. 2A), excluding the possibility of ectodermally Cre-induced phenotypes.

Next, to elucidate the function of AR expressed in the UPE, AR-floxed mice were crossed with Shh^{CreERT2} mice (hereafter referred to as epithelial ARKO). The UPE is derived from the endodermal cloacal epithelium where Shh is expressed (31). For the recombination of urethral epithelial cells, Shh^{CreERT2} embryos were treated with TM at E9.5. This treatment procedure was sufficient for the targeted recombination in the UPE (Fig. 2B). In the epithelial ARKO mice,

TABLE 1. The expression pattern of the Wnt ligands in the wild-type GTs at E15.5

	Gene expression	Primer sets
Wnt1	−	AAATGGCAATTCCGAAACCG/CGAAGATGAACGCTGTTTCTCG
Wnt2	+	AGATGTGATGCGTGCCATTG/CGATGCTGGCGGAACTG
Wnt2b	+	TACGGTGTTCGCTTTGCCA/TTCAGGAATCTCCGAACAGCC
Wnt3	−	GCCGCAATTACATCGAGATCAT/CCAGGCTGTCATCTATGGTGGT
Wnt3a	−	ATGTGAGCTCGCATGGCATAG/GACGTAGCAGCACCAATGGAA
Wnt4	+	CATCGAGGAGTGCCAATACCA/GACAGGGAGGGAGTCCAGTGT
Wnt5a	+	GCGTGGCTATGACCAGTTTAAGA/TTGACATAGCAGCACCAGTGAA
Wnt5b	+	TGTGGAGACAACGTGGAGTACG/TGTAGGTTCATGAGAGCTCGGC
Wnt6	−	GGTTTACACCAGCCCACGAA/GGAACTAGCAAAGGGCCTTTC
Wnt7a	+	CGCAAGCCCATGGACACT/GCCTGTCACTGGGTCCTCTTC
Wnt7b	+	CAATGGTGGTCTGGTACCCAAT/AGTCTCATGGTCCCTTTGTGGTT
Wnt8a	−	TCCGGCAGATGGGAAATTAC/TGGCGCTTGTCCATCTCAA
Wnt8b	−	CCCTGCCTTTCTCCGAAGAC/GCGGTGAAGGACACAAGTGA
Wnt9a	−	CGTGGGTGTGAAGGTGATAAAG/GCAGGAGCCAGACACACCAT
Wnt9b	+	GCTCAACGAGACCCCTAATATGTATAAG/TCAACCCTAGTTATGTTTATCTGAGTCTCAC
Wnt10a	−	CGGAACAAAGTCCCCTACGA/TGCTATGGCGTAGGCGAAAG
Wnt10b	+	ATGAGAGGTTTTCGGTTGGAAA/CCTCCCAAGAGCCTGACAAG
Wnt11	+	ATGTGCGGACAACCTCAGCTA/CGCATCAGTTTATTGGCTTGG
Wnt16	−	TGTATGGTCGCCACTACCACTT/GGTGCCGCTACTCAGCTCAT
Rspo1	−	TGTGAAATGAGCGAGTGGTCC/TCTCCCAGATGCTCCAGTTCT
Rspo2	−	TTGCATAGAGGCCGCTGCTTT/CTGGTCAGAGGATCAGGAATG
Rspo3	−	GTACACTGTGAGGCCAGTGAA/ATGGCTAGAACACCTGTCCTG
Rspo4	+	CTGGAGTCCCTGCATACACAA/CACGGGGAGAAGGAAAGTTTC

The expression of the Wnt ligands in the wild-type male GTs is assessed by RT-PCR. +, Presence of the corresponding gene expression; −, absence of an expression.

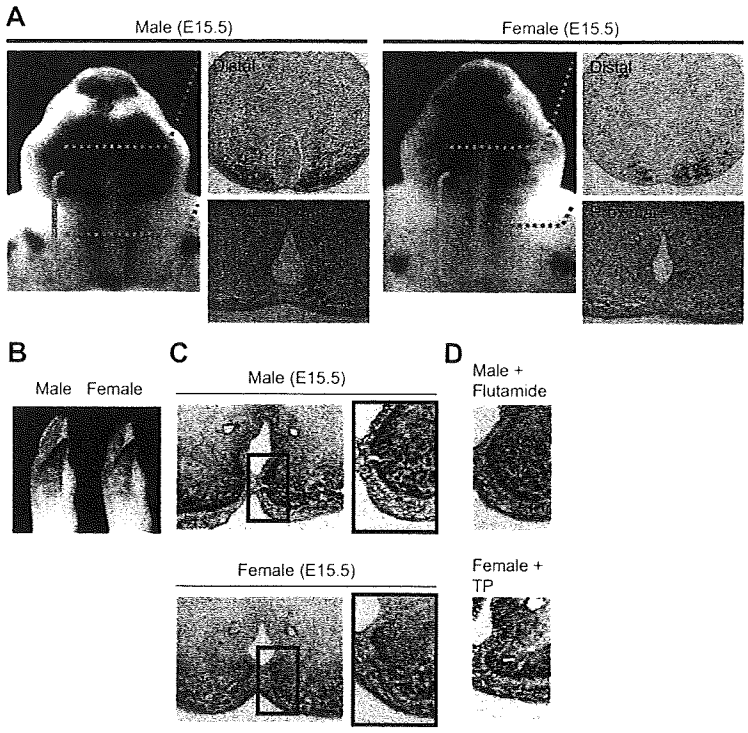

FIG. 4. Sexually dimorphic activity of Wnt/β-catenin signaling during GT development. A, The LacZ signal stained with the BatGAL line at E15.5. Note the enhanced LacZ signal in the male shown by the *red brackets* (shown in the high-magnitude pictures and in cross-sections for the distal and proximal region of the GT). B, In the limb, the sexually dimorphic pattern of the LacZ signal is not detected. C and D, Immunohistochemistry for anti-β-catenin antibodies in the GTs. β-Catenin is accumulated in the mesenchyme adjacent to the UPE in the male (*arrowheads*). Flutamide treatment represses β-catenin expression in the male embryos (D). In the GTs of female embryos treated with TP, β-catenin expression is increased in the mesenchyme when compared with those of control female (*arrows* in D).

more than 80% of cells in the endoderm display recombination (the recombination frequency was estimated by assessing the ratio of AR-positive cells in the endoderm), whereas the prominent AR expression in the mesenchyme is still detected (Fig. 2C, *right*). The mutants did not exhibit any abnormal GT phenotypes (10 embryos were examined; Fig. 2E), also indicating the essential roles of the mesenchymally expressed AR gene function for GT masculinization.

Sexually dimorphic activity of Wnt/β-catenin signaling in the developing GTs

After determining the critical timing and establishing a conditional gene-targeting strategy, the effector signal pathways for masculinization, estimated downstream targets of androgen, were analyzed. The sexually dimorphic expressing genes have been analyzed using a DNA microarray (32). Those analyses identified the expression of several Wnt inhibitory genes that were increased in the female GT at E15.5. The increased expression of Dkk (dickkopf) 2 and Sfrp (secreted frizzled-related protein) 1 in the female GTs in comparison with the males was confirmed by quantitative RT-PCR and *in situ* hybridization analyses (Fig. 3, A and B). To our knowledge, this could be the first case to demonstrate the sexually dimorphic expression of the Wnt signal genes. The expression of several Wnt ligand and R-spondin (Rspo) genes was also analyzed with RT-PCR (Table 1). Although a series of *in situ* gene expression and RT-PCR analyses were conducted for these genes in the sexually dimorphic stage of the GTs, prominent sexual dimorphisms were not detected in the current experimental conditions (data not shown).

To investigate the hormone dependency of Wnt inhibitory gene expression, a quantitative RT-PCR analysis was performed for Dkk2 and Sfrp1 in the female GTs treated with testosterone propionate and male GTs treated with flutamide (testosterone propionate or flutamide was treated at E15.5 and E16.5). Testosterone propionate treatment decreased the Dkk2 and Sfrp1 expression in the female GTs (Fig. 3A). Dkk2, but not Sfrp1, gene expression was increased by flutamide treatment in the male GTs (Fig. 3A). These data suggest that Dkk2 may be a novel and reliable feminized marker for GT development. In fact, Dkk2 expression was increased in the GTs of the mesenchymal ARKO mice in comparison with those of control males (Fig. 3A, and see also Fig. 5C).

The decreased level of Wnt inhibitory genes expressed in the male GTs could be associated with the sexually dimorphic Wnt/β-catenin activity. To investigate the presence of its signaling, the BatGAL mouse line, the Wnt/β-catenin signaling indicator mice, was analyzed (33). The LacZ signal derived from the BatGAL allele was detected in the mesenchymal cells adjacent to the UPE (Fig. 4A). This bilateral mesenchyme has been suggested to be essential for GT masculinization as shown above. This led to the examination of the sexually dimorphic activity of Wnt/β-catenin signaling during the GT masculinization processes. Notably, the LacZ signal derived from the BatGAL line was enhanced in the wild-type male GTs in comparison with those of the females (Fig. 4A). The LacZ signal in the limb, whose development is sex independent, was not altered (Fig. 4B). Next, the expression level of β-catenin was examined in the mesenchyme adjacent to the UPE of the male and female GTs. Consistent with the results of the Wnt/β-catenin signaling indicator mice, immunohistochemical analyses revealed that β-catenin accumulated in the mesenchymal cells of the male GTs in comparison with those of the female GTs (Fig. 4C). Notably, β-catenin expression level was decreased in the male embryos treated with flutamide and was increased in the female embryos treated with testosterone propionate (Fig. 4D). The above data all suggest that Wnt/β-catenin may function as one of the effector signals for androgen signaling in the male GTs.

Impaired sexual differentiation of external genitalia in loss- or gain-of-function mutants of β-catenin

Loss- or gain-of-function mutants of β-catenin were analyzed for the possible involvement of the Wnt/β-catenin activity for GT masculinization. To achieve the targeted gene recombination in the GT mesenchyme during the sexual developmental stage, the $Gli1^{CreERT2}$ line was treated with TM at E13.5. Under

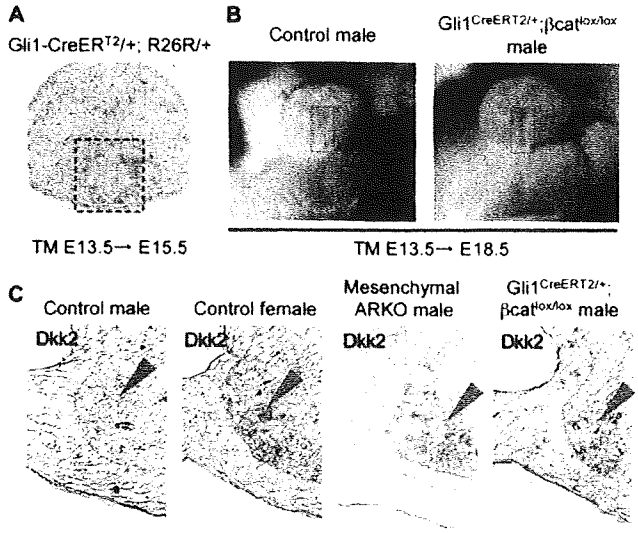

FIG. 5. Impaired GT development in the loss-of-function mutants of β-catenin. A, The Cre-mediated LacZ pattern in Gli1^{CreERT2} mice (crossed with R26R mice) treated with TM at E13.5 was examined at E15.5. The LacZ signal was detected in the mesenchyme adjacent to the UPE. B, The loss-of-function β-catenin mutants exhibit an unclosed prepuce at the midline of the male GT (*red boxes*). C, Dkk2 expression is increased in such genetic mutant male mice (*arrowheads*).

these conditions, recombined cells were observed in the mesenchyme adjacent to the UPE at E15.5, which is monitored by the R26R reporter allele (*boxed* region in Fig. 5A). Notably, this region overlaps with the region with the Wnt/β-catenin signal as shown by the BatGAL activity and β-catenin protein localization. This Cre mouse line was thus considered to be a useful tool to investigate the roles of Wnt/β-catenin signals during GT sexual development.

The β-catenin floxed mutant mice (β-catenin^{lox}), which contains two loxP sites that flank exons 3–6 (34), was first analyzed, and its conditional mutation in the mesenchyme during the GT masculinization stage was generated. In such a conditional loss-of-function mutant line, approximately 40% of the male embryos failed to develop the proper prepuce and ventral (lower) midline formation (seven of 18 embryos; Fig. 5B). Perturbed male GT development associated with a mesenchymal ARKO mutation or by Gli1$^{CreERT2/+}$;β-catenin$^{lox/lox}$ mutation was demonstrated by the increased Dkk2 expression, which is a feminized marker of the GTs (Fig. 5C). The GTs in the mutant females developed similarly to the control females (data not shown). These results suggest that β-catenin may be required for the ventral midline formation of the prepuce during male-type GT development.

Next, a constitutive active β-catenin^{loxEx3} mutant allele was analyzed to determine whether an enhanced Wnt/β-catenin signaling can masculinize the female GTs. Cre activity derived from the Gli1^{CreERT2} allele regulated by TM at E13.5 induces the constitutive active β-catenin that lacks the N-terminal domain phosphorylation sites essential for its degradation (35). The GTs of such compound mutant females showed well-developed prepuce in comparison with those of the control females at E18.5 (six of six embryos; Fig. 6A). This is similar to the phenotypes of the female embryos treated with androgens, which show prepuce hypertrophy adjacent to the midline seam sites (36). Some mutants can survive during the postnatal stage, and their adult external genital phenotypes (at postnatal d 35) were examined. Surprisingly, such adult mutant female mice exhibited a hyperplasic prepuce with enlarged external genitalia similar to the male GTs (Fig. 6B). The specificity of the phenotypes was confirmed by an analysis of the scrotum region. Indeed, such mutant mice still showed a prominent female-type perineum region in contrast to the male-type scrotum region (Fig. 6B).

Discussion

Mesenchymally expressed AR is indispensable for GT masculinization

The male and female external genitalia enable highly efficient fertilization in mammals. During embryogenesis, sexually dimorphic organogenesis is achieved by hormones produced in the gonads. Among such organs, the external genitalia develop from a single primordium, the GT. This bipotential nature of embryonic external genital development is particularly unique and therefore is a suitable model system to study developmental and reproductive biology.

The morphological sexual difference of the external genitalia is established at E16.5 in mice, at E17.5 in rat, and at 11–13 wk in humans (14, 37). An androgen-sensitive time window has been well documented by either antiandrogen or androgen exposure experiments in pregnant animals. According to such experiments, the androgen-sensitive window of sexual differentiation is indicated to be several days earlier than the morphologically dimorphic stages at E15-E19 in the rat and at 8–14 wk in humans (15). The current study identified the critical time point for the onset of sexually dimorphic development in mice as E15.5. The phenotype of the current genetically modified mice that were treated with TM at E13.5 showed sexual disorders.

A reciprocal interaction between the epithelium and mesenchyme is thought to be essential for urogenital organ development. For instance, mesenchymally expressed AR is required for the androgen-dependent epithelial cell differentiation in the prostate, another representative androgen target organ (38). In a reciprocal fashion, the epithelium is required for the differentiation and spatial organization of the smooth muscle in the prostate (39, 40). Previous tissue graft experiments demonstrated the inductive effects of the epithelium on mesenchymal growth and differentiation in the rat and mouse GTs (17, 28). However, the region-specific androgen function for GT masculinization has never been analyzed. In the current conditional ARKO mice study, the epithelially or mesenchymally specific functions of AR were genetically examined for the first time during GT development. AR was significantly expressed in the mesenchyme adjacent to the UPE, whereas such prominent AR expression was not detected in the mesenchymal ARKO mice. The current results demonstrate that the proper mesenchymal androgen signaling through its receptor is necessary for GT masculinization.

The androgen controls the GT masculinization hormonally during normal embryogenesis. In addition to androgen signaling

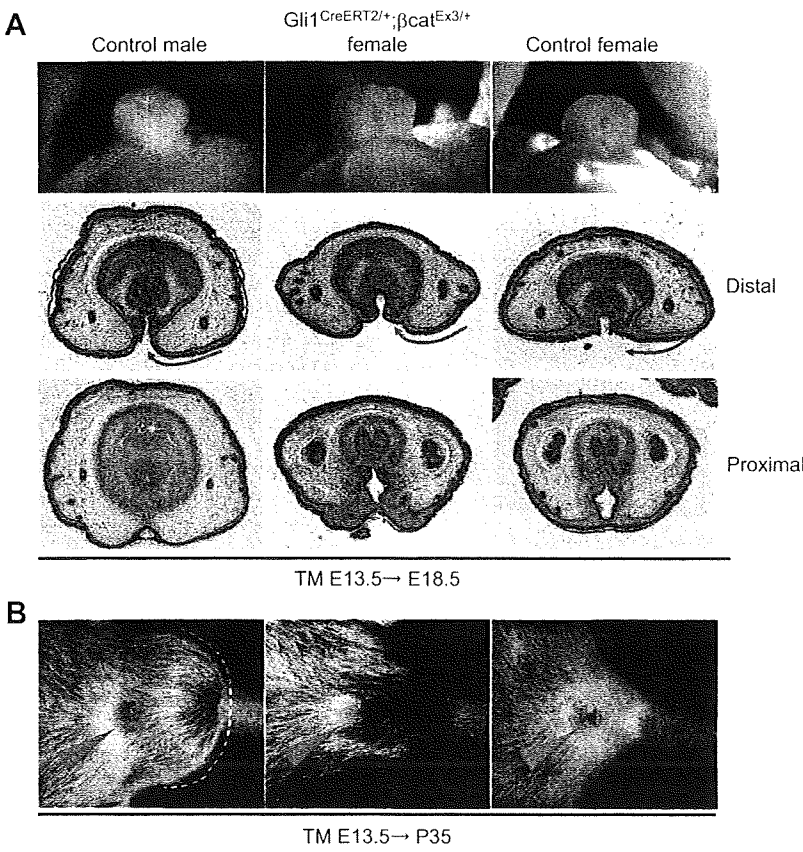

FIG. 6. Prepuce hyperplasia in the female GTs of the gain-of-function mutants of β-catenin. A, In the female GT with activated β-catenin in the mesenchyme, the prepuce exhibits hyperplasia. The histological sections corresponding to the levels of the distal GT represent preputial development to be accelerated in the constitutive active β-catenin mutants (*arrows*). B, Well-developed external genitalia observed in the gain-of-function β-catenin mutant female mice in comparison with those of the control female and male mice. Note that scrotal/perineal regions were not affected, showing the specificity of the resultant phenotypes. The *dotted line* indicates the scrotum.

through mesenchymally expressed AR, Wnt/β-catenin signaling in the mesenchyme is also essential for GT masculinization. Growth factor pathways have barely been identified as the effectors for reproductive organ masculinization including the GTs. Embryonic growth factor signaling has been generally suggested as the essential embryonic developmental program. Hence, mutations in such pathways have been considered to potentially induce an early embryonic lethality, masking their roles in the masculinization process. The current study identified several Wnt inhibitory genes that were decreasingly expressed in the male GTs in comparison with those in female GTs. Accompanying the decreased level of Wnt inhibitors, the β-catenin expression and BatGAL activity in the mesenchyme adjacent to the UPE was increased in the male GTs. Although sexually dimorphic expression of Wnt gene ligands and R-spondins was not detected in the GTs, it is possible that sexually dimorphic Wnt/β-catenin activity is elicited by combinational action of several Wnt gene ligands and their possible antagonists. In addition, loss- and gain-of-function studies for β-catenin demonstrated impaired sexual differentiation of the GTs. Of note is the fact that an activated β-catenin conditional mutant allele led to enlarged external genitalia in the XX female adult mice. These findings thus demonstrate the newly identified function of the Wnt/β-catenin signaling for embryonic masculinization, potentially functioning as a downstream effector of the androgen signaling.

It has been suggested that nuclear accumulation of β-catenin can be enhanced upon interacting with AR. Multiple findings have suggested an interaction between β-catenin and the AR, which is enhanced by the presence of an AR agonist (41, 42). Upon interacting with AR, β-catenin can translocate to the nucleus and affect AR-mediated transcriptional activities. In addition to the canonical β-catenin/Tcf/Lef pathway, it is thus also possible that β-catenin functions as a coactivator for AR enhancing GT masculinization. Further experiments are necessary to investigate such possibilities of β-catenin functions.

Considering the high incidence and an increasing prevalence of disorders of external genital development at birth, an understanding of their causative mechanisms and normal developmental process is vital in medical genetics. Effectors that mediate androgen signaling have not been identified so far. Various KO mouse studies demonstrated that defects in the initial outgrowth and patterning during the early morphogenesis stage induce severe lower (ventral) urethral groove defects or agenesis of the external genitalia (12). Generally, these defects can occur before androgen signaling genes are expressed. The current results demonstrate that abnormalities in Wnt/β-catenin signaling can not only affect early GT morphogenesis but also induce the embryonic masculinization disorders. A loss- and gain-of-function mutant mice for β-catenin showed early developmental anomalies, demonstrating a requirement of β-catenin during the early phase of GT development (25). However, it was previously not possible to analyze the roles for sexual development of the GTs. The current study took advantage of the TM-inducible Cre system and clearly demonstrated an essential role of β-catenin as a masculine effector of the GTs for the first time. Intriguingly, in the gonad, activation of β-catenin results in male-to-female sex reversal, suggesting that Wnt/β-catenin signaling is involved in the female pathway (43). Mice lacking Wnt4 or R-spondin1 genes exhibit a female-to-male sex-reversal in the gonads (44–46). Thus, β-catenin locates in the downstream of these genes (43). Hence, Wnt/β-catenin signaling is involved in sexual differentiation in a developmental context-dependent manner with different activities for male and female pathways.

The goal of the current study was to obtain a better understanding of the orchestrated signal networks essential for external genital masculinization. Little information about the integration of the signaling networks has been available for external

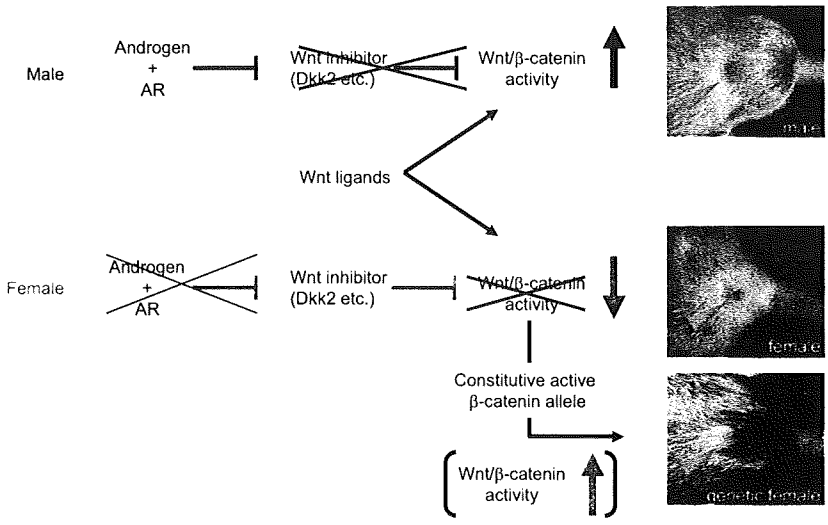

FIG. 7. A schematic diagram of the possible signaling cross talk among androgen and Wnt/β-catenin signaling for GT masculinization.

genital masculinization, to date. The study provided perspectives for normal reproductive biology and is also important for understanding the causative factors of the genital disorders. In summary, it is suggested that male GT development is regulated by Wnt/β-catenin signaling associated with the decreased expression levels of Wnt inhibitory genes, such as Dkk2 and Sfrp1. Wnt/β-catenin pathway exhibited thus sexually dimorphic activities, and their loss- and gain-of-function mutants displayed altered GT sexual development. These data suggest that the Wnt/β-catenin pathway can be a downstream effector of androgen signaling and an essential effector for GT masculinization (Fig. 7). The current results demonstrate that Wnt/β-catenin signaling is necessary for the orchestrated genital development and the masculinization of the external genitalia. To our knowledge, this could be the first genetic study analyzing the roles of the genetic interactions between androgen and locally expressed growth factor signaling during the development of reproductive organs.

Materials and Methods

Mouse and hormone treatments

The mutant alleles used herein were AR^{lox} (7), β-$catenin^{loxEx3}$ (35), β-$catenin^{lox}$ (34), K5-Cre (30), $Gli1^{CreERT2}$ (47), $Shh^{CreERT2}$ (48), R26R (49), and BatGAL (33). All experimental procedures and protocols were approved by the Committee on the Animal Research at the Kumamoto University. Embryos for each experiment were collected from more than three independent pregnant females. Statistical differences among the experimental groups were assessed by Fisher's exact probability test, and $P < 0.05$ was considered as statistically significant differences. Noon on the day when a vaginal plug was detected was designated as E0.5.

The TM-inducible Cre recombinase system removes the floxed sequence of the target genome (50). TM (Sigma Chemical Co., St. Louis, MO) was dissolved in sesame oil (Kanto Chemical, Tokyo, Japan) at a final concentration of 10 mg/ml. Four milligrams of TM per 40 g body weight was administered (ip) to the pregnant mice. For the Gli1-$CreER^{T2}$, β-$catenin^{loxEx3}$ mice, 2 mg TM per 40 g body weight was administered. Under these conditions, no overt teratological effects or sexual disorders of the reproductive organs were observed (29). To determine the critical time point of sexual differentiation of the GTs, pregnant C57BL/6 mice (CLEA, Tokyo, Japan) were given (ip) two successive injections of 100 mg/kg body weight flutamide or testosterone propionate (Sigma) dissolved in sesame oil.

Histology, X-gal staining, and immunohistochemistry

Hematoxylin and eosin staining and X-gal staining were performed by standard procedures as previously described (29). For immunohistochemistry, mouse embryos were fixed in 4% paraformaldehyde and embedded in paraffin. Deparaffinized sections were treated for antigen retrieval (microwave treatment 10 min in citrate buffer, pH 6.0) and incubated with 0.3% H_2O_2 in methanol for 10 min to eliminate endogenous peroxidases. The sections were incubated at a 1:200 dilution of anti-AR antibody (N-20; Santa Cruz Biotechnology, Santa Cruz, CA) and a 1:1000 dilution of anti-β-catenin antibody (clone 14; BD Biosciences, Franklin Lakes, NJ). After washing with PBS, the sections were stained with the Vectastain ABC Kit (Vector Laboratories, Burlingame, CA).

In situ hybridization for gene expression analysis

For *in situ* hybridization, paraformaldehyde-fixed, paraffin-embedded sections were deparaffinized, rehydrated, incubated in 1 μg/ml proteinase K for 7 min at 37 C, and refixed with 4% paraformaldehyde for 10 min at room temperature. After washing in PBS containing 0.1% Tween 20, overnight hybridization was performed in a buffer (50% formamide, 5× saline sodium citrate, 50 μg/ml yeast tRNA, 1% sodium dodecyl sulfate, 50 μg/ml heparin) with 1 μg/ml probe at 68 C. The slides were washed in 5× saline sodium citrate and 50% formamide for 1 h at 68 C, TBST buffer (140 mM NaCl, 2.7 mM KCl, 0.1% Tween 20, and 25 mM Tris-HCl, pH 7.5) for 5 min at room temperature before incubating for 2 h with blocking solution (10% blocking reagent (Roche, Mannheim, Germany) in 100 mM maleate buffer and TBST). Anti-digoxigenin antibody (Roche) in a blocking solution was added to the slides and incubated for 1 h. After washing with TBST, the sections were equilibrated in NTMT buffer (100 mM NaCl; 50 mM $MgCl_2$; 0.1% Tween 20; and 100 mM Tris-HCl, pH 9.5) including 2 mM levamisole (Sigma) and incubated in color solution containing 3.5 μg nitroblue tetrazolium (Roche) and 1.75 μg 5-bromo-4-chloro-3-indolyl phosphate (Roche) per milliliter of NTMT buffer.

The template used in this study was kindly provided from Dr. Christof Niehrs (Dkk2). The template of Sfrp1 was obtained by standard RT-PCR procedures. The primer sequences were TTC TAC ACC AAG CCC CCG CAG and GAT GGG CCC CAG CTT CAA GG. The preparation of the digoxigenin-labeled probes was performed according to the manufacturer's instructions (Roche).

Quantitative RT-PCR

The changes in gene expression were confirmed and quantified using the 7500 real-time PCR system (Applied Biosystems, Foster City, CA) according to the manufacturer's instructions. One microgram of total RNA, isolated with ISOGEN (Nippongene, Tokyo, Japan), was used in RT-PCR carried out with SuperScript III (Invitrogen, Carlsbad, CA) and SYBR Green master mix (Applied Biosystems). RNA from each group was purified from the mesenchyme adjacent to the UPE of the GTs (*blue area* shown in Fig. 3C). The relative RNA equivalents for each sample were determined by standardization with the ribosomal protein L8 levels. More than three pools of samples per group were tested in triplicate, and the average relative RNA equivalents per sample were used for further analysis. Error bars represent SE. The statistical comparisons

among the experimental groups were assessed by ANOVA. When F ratios were significant ($P < 0.05$), Scheffe *post hoc* tests between two groups were done, and $P < 0.05$ was considered as statistically significant differences. The primer sequences were as follows: Dkk2, TGT CTG AAG CAC AGG CTG GAT and CTT CTG GAG CCT CTG ATG GC; Sfrp1, AAG GAG AGG CAG AAT CCT TTC A and TTT CCA AAC CGG CCA ACA; and ribosomal protein L8, ACA GAG CCG TTG TTG GTG TTG and CAG CAG TTC CTC TTT GCC TTG T.

Acknowledgments

We thank Drs. A. Joyner, P. Chambon, A. McMahon, W. Birchmeier, T. Yamaguchi, C. Niehrs, H. Westphal, M. Renfree, A. Moon, S. Oottanmasathien, C. Mendelsohn, J. Takeda, T. Tsukiyama, S. Ohta, and L. Ma for materials and suggestions. We also express our appreciation T. Tanaka, C. Inoue, A. Omori, A. Murashima, K. Tanaka, C. Nakahara, H. Nishida, and S. Kitagawa for their assistance.

Address all correspondence and requests for reprints to: Gen Yamada, Center for Animal Resources and Development and Institute of Molecular Embryology and Genetics, Kumamoto University, Kumamoto 860-0811, Japan. E-mail: gensan@gpo.kumamoto-u.ac.jp.

This work was supported by Grant-in-Aid for Young Scientists B (19790153), Grant-in-Aid for Scientific Research B, Scientific Research on Priority Areas (Mechanisms of Sex Differentiation and General promotion of Cancer research in Japan), and the global COE program Cell Fate Regulation Research and Education Unit from the Ministry of Education, Culture, Sports, Science, and Technology, Japan, and a grant for Child Health and Development (17-2, 20-3) and Health Sciences Research Grant from the Ministry of Health, Labor, and Welfare, Japan. This work was also supported by National Institutes of Health Grant R01-ES016597-01A1.

Disclosure Summary: The authors have nothing to disclose.

References

1. Jost A 1953 Problems of fetal endocrinology: the gonadal and hypophyseal hormones. Recent Prog Horm Res 8:379–418
2. Baskin LS, Himes K, Colborn T 2001 Hypospadias and endocrine disruption: is there a connection? Environ Health Perspect 109:1175–1183
3. Boisen KA, Chellakooty M, Schmidt IM, Kai CM, Damgaard IN, Suomi AM, Toppari J, Skakkebaek NE, Main KM 2005 Hypospadias in a cohort of 1072 Danish newborn boys: prevalence and relationship to placental weight, anthropometrical measurements at birth, and reproductive hormone levels at three months of age. J Clin Endocrinol Metab 90:4041–4046
4. Skakkebaek NE, Rajpert-De Meyts E, Main KM 2001 Testicular dysgenesis syndrome: an increasingly common developmental disorder with environmental aspects. Hum Reprod 16:972–978
5. Clark AM, Garland KK, Russell LD 2000 Desert hedgehog (Dhh) gene is required in the mouse testis for formation of adult-type Leydig cells and normal development of peritubular cells and seminiferous tubules. Biol Reprod 63:1825–1838
6. Hammes A, Andreassen TK, Spoelgen R, Raila J, Hubner N, Schulz H, Metzger J, Schweigert FJ, Luppa PB, Nykjaer A, Willnow TE 2005 Role of endocytosis in cellular uptake of sex steroids. Cell 122:751–762
7. Sato T, Matsumoto T, Kawano H, Watanabe T, Uematsu Y, Sekine K, Fukuda T, Aihara K, Krust A, Yamada T, Nakamichi Y, Yamamoto Y, Nakamura T, Yoshimura K, Yoshizawa T, Metzger D, Chambon P, Kato S 2004 Brain masculinization requires androgen receptor function. Proc Natl Acad Sci USA 101:1673–1678
8. Yamada G, Satoh Y, Baskin LS, Cunha GR 2003 Cellular and molecular mechanisms of development of the external genitalia. Differentiation 71:445–460
9. Yong W, Yang Z, Periyasamy S, Chen H, Yucel S, Li W, Lin LY, Wolf IM, Cohn MJ, Baskin LS, Sánchez ER, Shou W 2007 Essential role for co-chaperone Fkbp52 but not Fkbp51 in androgen receptor-mediated signaling and physiology. J Biol Chem 282:5026–5036
10. Griffin JE, Leshin M, Wilson JD 1982 Androgen resistance syndromes. Am J Physiol 243:E81–E87
11. Wilson JD 1992 Syndromes of androgen resistance. Biol Reprod 46:168–173
12. Yamada G, Suzuki K, Haraguchi R, Miyagawa S, Satoh Y, Kamimura M, Nakagata N, Kataoka H, Kuroiwa A, Chen Y 2006 Molecular genetic cascades for external genitalia formation: an emerging organogenesis program. Dev Dyn 235:1738–1752
13. O'Shaughnessy PJ, Baker PJ, Johnston H 2006 The foetal Leydig cell: differentiation, function and regulation. Int J Androl 29:90–95; discussion 105–108
14. Suzuki K, Ogino Y, Murakami R, Satoh Y, Bachiller D, Yamada G 2002 Embryonic development of mouse external genitalia: insights into a unique mode of organogenesis. Evol Dev 4:133–141
15. Welsh M, Saunders PT, Fisken M, Scott HM, Hutchison GR, Smith LB, Sharpe RM 2008 Identification in rats of a programming window for reproductive tract masculinization, disruption of which leads to hypospadias and cryptorchidism. J Clin Invest 118:1479–1490
16. Kurzrock EA, Baskin LS, Cunha GR 1999 Ontogeny of the male urethra: theory of endodermal differentiation. Differentiation 64:115–122
17. Kurzrock EA, Baskin LS, Li Y, Cunha GR 1999 Epithelial-mesenchymal interactions in development of the mouse fetal genital tubercle. Cells Tissues Organs 164:125–130
18. Haraguchi R, Mo R, Hui C, Motoyama J, Makino S, Shiroishi T, Gaffield W, Yamada G 2001 Unique functions of Sonic hedgehog signaling during external genitalia development. Development 128:4241–4250
19. Haraguchi R, Suzuki K, Murakami R, Sakai M, Kamikawa M, Kengaku M, Sekine K, Kawano H, Kato S, Ueno N, Yamada G 2000 Molecular analysis of external genitalia formation: the role of fibroblast growth factor (Fgf) genes during genital tubercle formation. Development 127:2471–2479
20. Morgan EA, Nguyen SB, Scott V, Stadler HS 2003 Loss of Bmp7 and Fgf8 signaling in Hoxa13-mutant mice causes hypospadia. Development 130: 3095–3109
21. Perriton CL, Powles N, Chiang C, Maconochie MK, Cohn MJ 2002 Sonic hedgehog signaling from the urethral epithelium controls external genital development. Dev Biol 247:26–46
22. Petiot A, Perriton CL, Dickson C, Cohn MJ 2005 Development of the mammalian urethra is controlled by Fgfr2-IIIb. Development 132:2441–2450
23. Suzuki K, Bachiller D, Chen YP, Kamikawa M, Ogi H, Haraguchi R, Ogino Y, Minami Y, Mishina Y, Ahn K, Crenshaw 3rd EB, Yamada G 2003 Regulation of outgrowth and apoptosis for the terminal appendage: external genitalia development by concerted actions of BMP signaling. Development [Erratum (2003) 130:6643] 130:6209–6220
24. Yamaguchi TP, Bradley A, McMahon AP, Jones S 1999 A Wnt5a pathway underlies outgrowth of multiple structures in the vertebrate embryo. Development 126:1211–1223
25. Lin C, Yin Y, Long F, Ma L 2008 Tissue-specific requirements of β-catenin in external genitalia development. Development 135:2815–2825
26. Prins GS, Putz O 2008 Molecular signaling pathways that regulate prostate gland development. Differentiation 76:641–659
27. Wilson JD, Griffin JE, George FW, Leshin M 1983 The endocrine control of male phenotypic development. Aust J Biol Sci 36:101–128
28. Murakami R, Mizuno T 1986 Proximal-distal sequence of development of the skeletal tissues in the penis of rat and the inductive effect of epithelium. J Embryol Exp Morphol 92:133–143
29. Haraguchi R, Motoyama J, Sasaki H, Satoh Y, Miyagawa S, Nakagata N, Moon A, Yamada G 2007 Molecular analysis of coordinated bladder and urogenital organ formation by Hedgehog signaling. Development 134:525–533
30. Tarutani M, Itami S, Okabe M, Ikawa M, Tezuka T, Yoshikawa K, Kinoshita T, Takeda J 1997 Tissue-specific knockout of the mouse Pig-a gene reveals important roles for GPI-anchored proteins in skin development. Proc Natl Acad Sci USA 94:7400–7405
31. Seifert AW, Harfe BD, Cohn MJ 2008 Cell lineage analysis demonstrates an endodermal origin of the distal urethra and perineum. Dev Biol 318:143–152
32. Nishida H, Miyagawa S, Matsumaru D, Wada Y, Satoh Y, Ogino Y, Fukuda S, Iguchi T, Yamada G 2008 Gene expression analyses on embryonic external genitalia: identification of regulatory genes possibly involved in masculinization processes. Congenit Anom (Kyoto) 48:63–67
33. Nakaya MA, Biris K, Tsukiyama T, Jaime S, Rawls JA, Yamaguchi TP 2005 Wnt3a links left-right determination with segmentation and anteroposterior axis elongation. Development 132:5425–5436
34. Huelsken J, Vogel R, Erdmann B, Cotsarelis G, Birchmeier W 2001 β-Catenin controls hair follicle morphogenesis and stem cell differentiation in the skin. Cell 105:533–545
35. Harada N, Tamai Y, Ishikawa T, Sauer B, Takaku K, Oshima M, Taketo MM 1999 Intestinal polyposis in mice with a dominant stable mutation of the β-catenin gene. EMBO J 18:5931–5942

36. Yucel S, Cavalcanti AG, Desouza A, Wang Z, Baskin LS 2003 The effect of oestrogen and testosterone on the urethral seam of the developing male mouse genital tubercle. BJU Int 92:1016–1021
37. Reyes FI, Winter JS, Faiman C 1973 Studies on human sexual development. I. Fetal gonadal and adrenal sex steroids. J Clin Endocrinol Metab 37:74–78
38. Cunha GR, Chung LW, Shannon JM, Reese BA 1980 Stromal-epithelial interactions in sex differentiation. Biol Reprod 22:19–42
39. Cunha GR, Battle E, Young P, Brody J, Donjacour A, Hayashi N, Kinbara H 1992 Role of epithelial-mesenchymal interactions in the differentiation and spatial organization of visceral smooth muscle. Epithelial Cell Biol 1:76–83
40. Hayward SW, Haughney PC, Rosen MA, Greulich KM, Weier HU, Dahiya R, Cunha GR 1998 Interactions between adult human prostatic epithelium and rat urogenital sinus mesenchyme in a tissue recombination model. Differentiation 63:131–140
41. Mulholland DJ, Dedhar S, Coetzee GA, Nelson CC 2005 Interaction of nuclear receptors with the Wnt/β-catenin/Tcf signaling axis: Wnt you like to know? Endocr Rev 26:898–915
42. Verras M, Sun Z 2006 Roles and regulation of Wnt signaling and β-catenin in prostate cancer. Cancer Lett 237:22–32
43. Maatouk DM, DiNapoli L, Alvers A, Parker KL, Taketo MM, Capel B 2008 Stabilization of β-catenin in XY gonads causes male-to-female sex-reversal. Hum Mol Genet 17:2949–2955
44. Chassot AA, Ranc F, Gregoire EP, Roepers-Gajadien HL, Taketo MM, Camerino G, de Rooij DG, Schedl A, Chaboissier MC 2008 Activation of β-catenin signaling by Rspo1 controls differentiation of the mammalian ovary. Hum Mol Genet 17:1264–1277
45. Tomizuka K, Horikoshi K, Kitada R, Sugawara Y, Iba Y, Kojima A, Yoshitome A, Yamawaki K, Amagai M, Inoue A, Oshima T, Kakitani M 2008 R-spondin1 plays an essential role in ovarian development through positively regulating Wnt-4 signaling. Hum Mol Genet 17:1278–1291
46. Vainio S, Heikkila M, Kispert A, Chin N, McMahon AP 1999 Female development in mammals is regulated by Wnt-4 signalling. Nature 397:405–409
47. Ahn S, Joyner AL 2004 Dynamic changes in the response of cells to positive hedgehog signaling during mouse limb patterning. Cell 118:505–516
48. Harfe BD, Scherz PJ, Nissim S, Tian H, McMahon AP, Tabin CJ 2004 Evidence for an expansion-based temporal Shh gradient in specifying vertebrate digit identities. Cell 118:517–528
49. Soriano P 1999 Generalized lacZ expression with the ROSA26 Cre reporter strain. Nat Genet 21:70–71
50. Feil R, Wagner J, Metzger D, Chambon P 1997 Regulation of Cre recombinase activity by mutated estrogen receptor ligand-binding domains. Biochem Biophys Res Commun 237:752–757

Ecotoxicology and Environmental Safety 72 (2009) 1400–1405

Contents lists available at ScienceDirect

Ecotoxicology and Environmental Safety

journal homepage: www.elsevier.com/locate/ecoenv

Application of metamorphosis assay to a native Japanese amphibian species, *Rana rugosa*, for assessing effects of thyroid system affecting chemicals

Tomohiro Oka [a], Maki Miyahara [a], Jun Yamamoto [a], Naoko Mitsui [a], Takaaki Fujii [b], Osamu Tooi [a], Keiko Kashiwagi [c], Minoru Takase [c], Akihiko Kashiwagi [d], Taisen Iguchi [e,*]

[a] *Institute of Environmental Ecology, IDEA Consultants, Inc., 1334-5 Riemon, Yaizu, Shizuoka 421-0212, Japan*
[b] *Technology Center, Towa Environment Science Co., Ltd., Dejima, Minamiku, Hiroshima, Japan*
[c] *Institute for Amphibian Biology, Graduate School of Science, Hiroshima University, 1-3-1 Kagamiyama, Higashihiroshima, Hiroshima 739-8526, Japan*
[d] *Sanyo Women's College, 1-1 Sagatahonmachi, Hatsukaichi, Hiroshima 738-8504, Japan*
[e] *Division of Bio-Environmental Science, Department of Bio-Environmental Science, Okazaki Institute for Integrative Bioscience, National Institute for Basic Biology, National Institutes of Natural Sciences, 5-1 Higashiyama, Myodaiji, Okazaki, Aichi 444-8787, Japan*

ARTICLE INFO

Article history:
Received 13 January 2009
Received in revised form
27 March 2009
Accepted 30 March 2009
Available online 25 April 2009

Keywords:
Rana rugosa
Xenopus laevis
Xenopus (Silurana) tropicalis
Amphibian metamorphosis assay
Thyroid hormone
Propylthiouracil
Endocrine disruptors

ABSTRACT

The aims of this study were to assess the utility of a metamorphosis assay for detecting thyroid hormone-disrupting chemicals using *Rana rugosa*, a domestic frog species in Japan, and to compare species differences in sensitivity to thyroxine (T_4) and propylthiouracil (PTU) among *R. rugosa*, *Xenopus laevis* and *Xenopus (Silurana) tropicalis*. Tadpoles of *R. rugosa* (TK stages III/IV) were exposed to standard test chemicals for acceleration (T_4) and inhibition (PTU) of metamorphosis for 28 days in semi-static condition and total body length and developmental stage (TK stage) were recorded every week. T_4 (0.61 and 2.24 μg/L in actual concentrations) and PTU (19.73, 76.83, and 155.67 mg/L in actual concentrations) induced significant acceleration and inhibition of metamorphosis, respectively. The present results indicate that the metamorphosis assay is successfully applied to the domestic frog species, *R. rugosa*, suggesting this assay can be used for the assessment of chemicals on ecological impacts in wild frog species.

1. Introduction

A large number of chemicals in the environment have the potential to disrupt endocrine systems in vertebrates (**Colborn et al., 1993**). Some chemicals have potential to cause adverse effects on reproductive development and function in wildlife by disrupting the endocrine system (**Colborn, 1995**; **Tyler et al., 1998**). For the detection and characterization of environmental chemicals with potential thyroid-disrupting activities, the amphibian metamorphosis assay was selected by the OECD Task Force on Endocrine Disrupters Testing and Assessment (EDTA) as an *in vivo* assay (**OECD, 2003**; **Opitz et al., 2005**). *Xenopus laevis* has been used as a test animal for the metamorphosis assay for detecting chemicals with agonistic and antagonistic activities of thyroid hormone, since the metamorphosis induced by thyroid hormone has been well characterized in this species (**Goleman et al., 2002**; **Kloas et al., 2002, 2003**; **Degitz et al., 2005**; **Opitz et al., 2005**; **Tata, 2006**). A current study demonstrated that the metamorphosis assay was successfully applied to *Xenopus (Silurana) tropicalis* (**Mitsui et al., 2006**). *X. tropicalis* offers some advantages over *X. laevis* as a model animal, including diploid vs. tetraploid genome (**Amaya et al., 1998**; **Hirsch et al., 2002**; **Gilchrist et al., 2004**), and its shorter life cycle is likely to be advantageous in chronic ecotoxicity testing, for example, for endocrine disrupting chemicals. Both these species can be used in metamorphosis assays for detecting thyroid hormone disrupters. In addition, the development of a comparable test protocol for domestic species will lend greater support to ecological risk assessment of chemicals.

The wrinkled frog, *Rana rugosa*, is distributed as a domestic species in Japan (**Maeda and Matsui, 2003**). *R. rugosa* has been frequently used to study sex lampbrush chromosomes, evolution of heterogametic sex, and sex determination (**Miura et al., 1996, 1997, 1998**; **Kato et al., 2004**). Effects of thyroid hormone and its antagonist on tail resorption have been reported in *R. rugosa* (**Hanada et al., 2003**; **Kitamura et al., 2005**; **Goto et al., 2006**); however, no common protocol for a metamorphosis assay has been established.

In the present study, *X. laevis* metamorphosis assay (XEMA) protocol (**Opitz et al., 2005**) was applied to a domestic species in

* Corresponding author. Fax: +81 564 59 5236.
E-mail address: **taisen@nibb.ac.jp** (T. Iguchi).

0147-6513/$ - see front matter © 2009 Elsevier Inc. All rights reserved.
doi:10.1016/j.ecoenv.2009.03.012

Japan, *R. rugosa*, for the first time, to establish detailed protocol of metamorphosis assay for this species.

2. Materials and methods

2.1. Chemicals

Thyroxine (T_4; CAS 51-48-9) and propylthiouracil (PTU; 6-n-propyl-2-thiouracil; CAS 51-52-5) were obtained from Sigma Chemical Co. (St. Louis, MO, USA) at the highest purity available. Stock solutions of T_4 and PTU were prepared in 0.1 M NaOH and 0.7 M NaOH, respectively. All experimental aspects were conducted in compliance with the institutional guidelines for the care and use of animals.

2.2. Preparation of tadpoles

R. rugosa embryos were supplied from the Institute for Amphibian Biology, Hiroshima University. Ovulation was induced by an injection using suspension of crushed pituitaries of *Rana catesbeiana* (bull frog) into the body cavity of *R. rugosa* females. Eggs were collected from females and artificially fertilized with suspension of crushed testes. Embryos were transferred into the test medium consisting of 0.25 g/L commercial salt mixture, Tropic Marin Meersalz (Dr. Biener GmbH, Wartenberg, Germany), pH 7.0±0.5, in deionized aerated water. Embryos were developed at 22, 25, and 28 °C in each experiment.

The normal development of *R. rugosa* tadpoles was staged according to Taylor and Kollros (1946) (TK stage), which is the normal table of *Rana pipiens*. The normal table was compared with the normal table of *X. laevis* established by Nieuwkoop and Faber (1994).

2.3. Experiments

2.3.1. Effect of rearing temperature

Initially, the optimal temperature for rearing tadpoles of *R. rugosa* was investigated. Ten embryos were assigned to each of six test vessels (glass aquaria, 22 × 25 × 30 cm), which were filled with 3.3 L of aerated test medium at three temperatures (22, 25, and 28 °C). Cohorts of tadpoles developed in duplicate tanks per temperature for 7 weeks after fertilization. Tadpoles were fed boiled spinach daily (0.2–0.5 g per tank) and maintained in 12-h light/12-h dark photoperiod. The test medium was changed three times per week (i.e. tadpoles were reared in semi-static conditions). Time to metamorphosis of developing tadpoles was recorded weekly from weeks 3 to 7. Determination of developmental stage was performed under a stereo-microscope according to TK stage.

2.3.2. Metamorphosis assay

A metamorphosis assay using *R. rugosa* was performed based on the *X. laevis* metamorphosis assay (Kloas et al., 2003; Opitz et al., 2005). Tadpoles were reared in test medium at 25 °C during the pre-exposure phase for 3 weeks, and then 10 tadpoles were placed in each test vessel (glass aquaria, 22 cm × 25 cm × 30 cm) containing 3.3 L of test medium at TK stages III/IV, which corresponds to stages 49–51 of *X. laevis* (Nieuwkoop and Faber, 1994). Tadpoles were exposed to 0.25, 1.0, and 4.0 μg/L (0.32, 1.29, and 5.15 nM) T_4 in nominal concentration, as positive controls for thyroid hormone agonistic activity (2 tanks per concentration) and 18.75, 75, and 150 mg/L (0.11, 0.44, and 0.88 mM) PTU in nominal concentration, as positive controls for anti-thyroid hormone activity (2 tanks per concentration), or test medium alone (3 tanks for controls). Tadpoles were exposed for 28 days under semi-static conditions in a 12-h light/12-h dark photoperiod. All tadpoles were fed boiled spinach, and total daily food ratio was increased along with tadpole growth, approximately 0.2–0.5 g/tadpole through the course of the study. Test medium in all tanks was changed completely three times a week. During the test duration, the tadpoles were checked daily for mortality, and developmental (TK) stage and total body length were measured and recorded weekly. A caliper was used to measure the total body length of the tadpole. Determination of developmental stage was performed under a stereo-microscope according to TK stage.

2.4. Histology

Five tadpoles exposed to T_4 and controls were harvested, and were anaesthetized on ice when metamorphosis had been completed (5–7 weeks after exposure). Since PTU-exposed tadpoles did not complete the metamorphosis, tadpoles (five samples) were harvested 12 weeks after exposure. The whole body including thyroid glands was fixed in Neofix (Merck, Darmstadt, Germany), dehydrated and embedded in paraffin. Tadpoles were placed in ventral recumbency and decapitated in a plane perpendicular to the caudal-rostral axis. Five-step sections were taken from each block, and two serial sections of each step are placed. Sections were cut at 6 μm thickness and stained with hematoxylin and eosin. Sections in each sample were acquired from the central portions of the thyroid glands to provide an accurate reflection of thyroid size (OECD, 2007), and thyroid glands were observed pathological changes such as hypertrophy, atrophy, follicular cell hypertrophy, and follicular cell hyperplasia including histological endpoints selected in the OECD amphibian metamorphosis assay (OECD, 2007; Grim et al., 2009). A section of the largest thyroid gland including the middle area of thyroid gland was selected and observed.

2.5. Chemical measurement

Chemical analysis of T_4 and PTU in the test medium was carried out using high-performance liquid chromatography (HPLC)–mass spectrometry (MS). T_4 and PTU concentrations were measured twice. The first sample was taken immediately after chemical exposure to the test medium (fresh water after medium exchange) and the second was taken from the test vessels before test medium exchange to determine the relative quantity of T_4 and PTU remaining (water sample at 2 days after exposure with the test medium containing tadpoles and feed). Water samples were maintained in glass bottles at −30 °C until analysis.

For measurement of actual T_4 concentrations in the test medium, water samples (50–200 mL) were diluted in methanol. Each sample was loaded on PS-2 cartridges (Waters, MA, USA), which were conditioned with methanol and double-distilled water (DDW) in advance. T_4 was extracted from the cartridge with methanol at a flow rate of 10 mL/min, and then the eluted T_4 was reconstituted in 1 mL by methanol purging with N_2. Each aliquot of the sample (5 μL) was injected into HPLC (Agilent 1100, Agilent Technologies, Tokyo, Japan) housing a Mightysil Rp-18 GP (2.0 mm × 150 mm) column (Kanto Chemical Co. Inc., Tokyo, Japan). The oven temperature was 40 °C during the injection. The column was eluted with 0.1% formic acid: methanol gradient programmed from 50% to 70% of methanol for 15 min at a flow rate of 0.2 mL/min, and the post-column reagent is determined at *m/z* of 778.6 by the API-400 Q-Trap MS system (Applied Biosystems Inc., CA, USA). The recovery ratio of standard T_4 (0.2 μg/L) in this method was 79.5% of nominal concentration.

Water samples (50 mL) from test vessels containing PTU were diluted in methanol. In total 5 μL of each sample was injected into a Develosil C30-UG-5 (2.0 mm × 150 mm) column (Nomura Chemical Co., Ltd., Aichi, Japan). The column was maintained at 40 °C during the injection, and then eluted with 0.1% formic acid: methanol gradient programmed from 0% to 60% of methanol for 12 min at a flow rate of 0.2 mL/min. The post-column reagent was analyzed by the MS system, and then determined at an *m/z* of 171.1. The recovery ratio of standard PTU (100 μg/L) in this method was 99.7% of nominal concentration.

2.6. Statistical analyses

Statistical analyses were performed according to the XEMA ring-test (Opitz et al., 2005). The normal development of *R. rugosa* tadpoles was staged according to the normal table of *R. pipiens* by Taylor and Kollros (1946) (TK stage), which is indicated by Roman letters. Consequently, these data were converted to Arabic numbers prior to statistical analysis of the developmental-stage parameter. Non-parametric Kruskal–Wallis test followed by Dunn's test was used to determine differences for the developmental stage exhibited between each exposure group and control. Total body length data were analyzed for normal distribution (Kolmogorov and Smirnov test) and homogeneity of variance (Levene test) by each day was recorded. For normally distributed data, Dunnett's test was performed for difference compared from the control group to all exposure groups. For data not meeting criteria of normality and homogeneity of variance, non-parametric Kruskal–Wallis test followed by Dunn's test was used. These statistical analyses were conducted with Stat Light Software (Yukms Co. Ltd., Tokyo, Japan) and SPSS software (SPSS Japan Inc., Tokyo, Japan).

3. Results

3.1. Effects of rearing temperature on R. rugosa development and metamorphosis

The effect of temperature on metamorphosis was assessed in *R. rugosa* to inform our selection of test temperature for the XEMA-type metamorphosis assay. Embryos at all temperatures, 22, 25, and 28 °C, developed successfully for 7 weeks after fertilization. After 3 weeks, tadpoles reared at 25 and 28 °C reached stages III/IV. Between weeks 4 and 7, significant acceleration of development was observed in tadpoles reared at 25 and 28 °C, compared to those at 22 °C (Fig. 1). No tadpole mortalities were observed in the course of the study.

3.2. Metamorphosis assay

The metamorphosis assay using *R. rugosa* was carried out to assess the suitability of *R. rugosa* for a metamorphosis assay resembling that of the XEMA test developed in *X. laevis* for detection of chemicals having thyroid hormone-disrupting activities. The test was initiated with *R. rugosa* tadpoles at TK stages III/IV, which is functionally equivalent to stages 49–51 (**Nieuwkoop and Faber, 1994**) in *X. laevis*. These tadpoles were measured and recorded for total body length and developmental stage weekly until the termination of test at 28 days after exposure.

3.2. 1. Chemical analysis of T_4 and PTU

Three concentrations of T_4 (0.25, 1.0, and 4.0 μg/L) were used as positive controls for thyroid hormone activity (**Opitz et al., 2005**). Actual T_4 concentrations in the test medium were measured using HPLC-MS (**Table 1**). Fresh water samples were taken immediately after medium exchange to the test medium. Actual concentrations of T_4 were 0.16 (64.0%) μg/L, 0.61 (61.0%) μg/L, and 2.24 (56.0%) μg/L for nominal concentrations of 0.25, 1.0, and 4.0 μg/L T_4, respectively. The actual concentrations of T_4 at 2 days after exposure, which is the sample taken before test medium exchange to determine the relative quantity of T_4 remaining, were 0.06 (24.0%) μg/L, 0.15 (15.0%) μg/L, and 0.94 (23.5%) μg/L for the nominal concentrations of 0.25, 1.0, and 4.0 μg/L, respectively.

Three concentrations of PTU (18.75, 75, and 150 mg/L) were used as a positive control for anti-thyroid hormone activity for 28 days (**Opitz et al., 2005**). The actual concentrations of PTU immediately after exposure to the test medium were 19.73 (105.2%), 76.83 (102.4%), and 155.67 (103.8%) mg/L for nominal concentrations of 18.75, 75, and 150 mg/L, respectively, while the concentrations at 2 days after exposure in each PTU exposure group were 19.34 (103.1%), 75.6 (100.8%), and 153.38 (102.3%) mg/L of the respective nominal concentrations (**Table 1**).

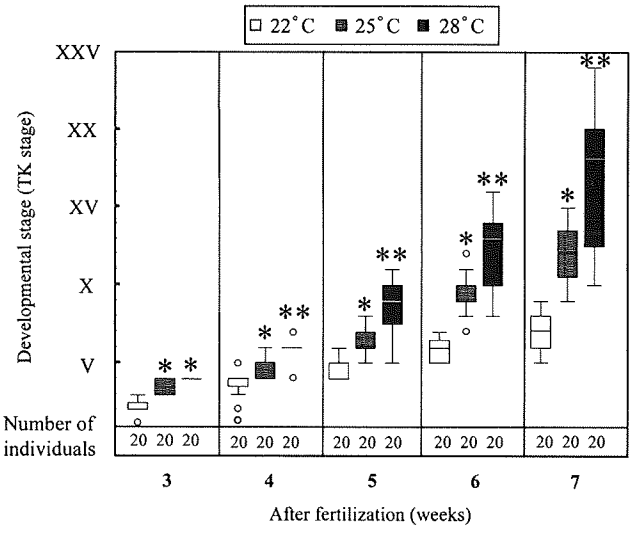

Fig. 1. Effect of rearing temperature on developmental stage. *Rana rugosa* tadpoles were reared at 22, 25, and 28 °C. Bars indicate median values, and boxes demarcate 25th and 75th percentiles. The extreme values (within 1.5-fold boxes) are the ends of the lines extending from the boxes. Points at a greater distance from the extreme values were indicated as open circles. The numbers of tadpoles surviving and measured are listed in the figure. *$P<0.05$ vs. respective tadpoles at 22 °C (Dunn's test). **$P<0.05$ vs. 22 and 25 °C groups (Dunn's test).

Table 1
Chemical analysis of T_4 and PTU in the test medium using HPLC–MS.

Chemicals (nominal concentrations)	Actual concentrations in test medium (recovery ratio, %)	
	Fresh water samples[a]	Samples at 2 days after exposure[b]
T_4 (0.25 μg/L)	0.16 μg/L (64%)	0.06 μg/L (24%)
T_4 (1.0 μg/L)	0.61 μg/L (61%)	0.15 μg/L (15%)
T_4 (4.0 μg/L)	2.24 μg/L (56%)	0.94 μg/L (23.5%)
PTU (18.75 mg/L)	19.73 mg/L (105.2%)	19.34 mg/L (103.1%)
PTU (75 mg/L)	76.83 mg/L (102.4%)[a]	75.6 mg/L (100.8%)
PTU (150 mg/L)	155.67 mg/L (103.8%)[a]	153.8 mg/L (102.3%)

[a] The sample was taken immediately after chemical exposure to the test medium (fresh water).

[b] The sample was taken from the test vessels before test medium exchange to determine the relative quantity of T_4 and PTU remaining (water sample at 2 days after medium exchange).

3.2.2. Control

Thirty tadpoles in total (3 tanks with 10 tadpoles per tank) were used as the controls. Control tadpoles reached stages XIII–XVII at the termination of the assay, being 28 days after exposure (**Figs. 2 and 3**). The median developmental stage for controls at day 28 was stage XIV, which corresponded approximately to stage 57 in *X. laevis*. No external malformation was noted during the test period, but there was one (unexplained) mortality among the controls (3.3%) (**Table 2**). The growth of tadpoles was assessed by means of total body length (Table 3). In the control group, mean total body length was increased by 28 days after exposure, reaching 42–43 mm in the largest tadpoles.

3.2.3. Thyroxine (T_4)

Twenty tadpoles in total were assessed in each exposure group. Tadpoles exposed to 0.61 and 2.24 μg/L T_4 exhibited acceleration of metamorphic development, as compared to the control group at days 14–28 and days 7–14, respectively (**Fig. 2**). In the tadpoles exposed to 0.16 μg/L T_4, developmental stage was significantly enhanced at day 21 of exposure, but not at day 28 (**Fig. 2**). Total body length in 0.61 and 2.24 μg/L T_4-exposed tadpoles was

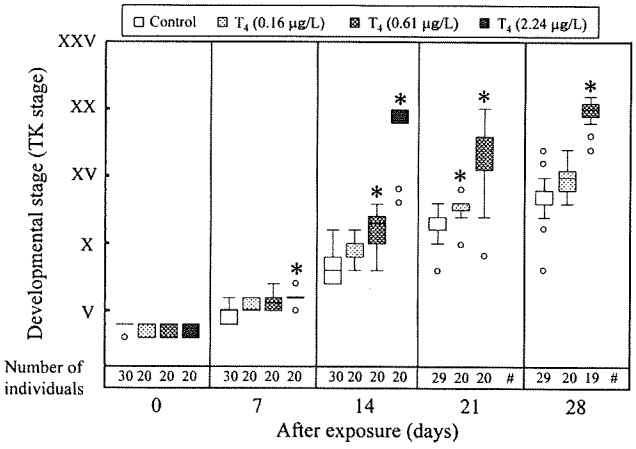

Fig. 2. Distribution of developmental (TK) stage of *R. rugosa* tadpoles in control group and T_4 groups, assessed every 7 days during the test period. Bars indicate median values, and boxes demarcate 25th and 75th percentiles. The extreme values (within 1.5-fold boxes) are the ends of the lines extending from the boxes. Points at a greater distance from the extreme values were indicated as open circles. The numbers of tadpoles surviving and measured are listed in the figure. #All tadpoles in this treatment group died during the study or exhibited malformation. *$P<0.05$ vs. respective controls (Dunn's test).

significantly shorter than the controls at day 28 and day 14, respectively, while the tadpoles exposed to 0.16 μg/L T_4 showed no difference (**Table 3**). The mortalities in 0.16 and 0.61 μg/L T_4 groups were 0% and 5%, respectively. No malformation was observed in tadpoles exposed to 0.16 and 0.61 μg/L T_4. In the present study, all tadpoles exposed to 2.24 μg/L T_4 exhibited abnormalities such as short tail, swollen abdomen, and immature limb at day 14, and these tadpoles were all dead by day 21 (**Table 2**). Moreover, the effects of T_4 on thyroid gland by histological analysis were examined for five tadpoles in each group. The size of thyroid gland in 0.16 and 0.61 μg/L T_4-exposed tadpoles of completed metamorphosis was smaller than that of controls of completed metamorphosis (**Fig. 4**). The effects of T_4 on thyroid gland were observed in two of five tadpoles and all five tadpoles exposed to 0.16 and 0.61 μg/L, respectively.

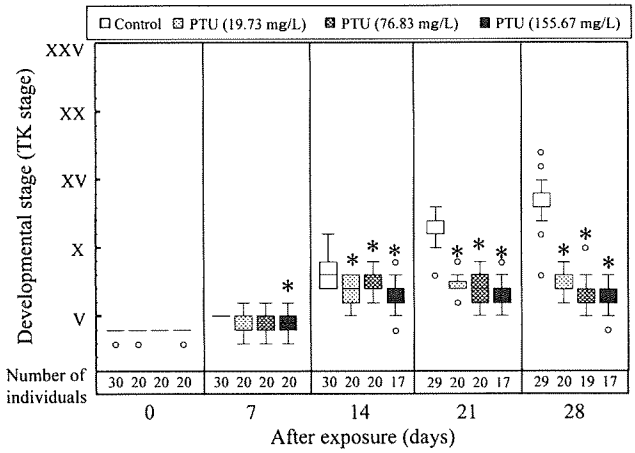

Fig. 3. Distribution of developmental stage of *R. rugosa* tadpoles in control group and PTU groups. The developmental stage of *R. rugosa* tadpole was assessed by median of stage determination according to TK stage. Bars indicate median values, and boxes demarcate 25th and 75th percentiles. The extreme values (within 1.5-fold boxes) are the ends of the lines extending from the boxes. Points at a greater distance from the extreme values were indicated as open circles. The numbers of tadpoles surviving and measured are listed in the figure. *$P<0.05$ vs. respective controls (Dunn's test).

3.2.4. *Propylthiouracil*

In the present study, PTU inhibited metamorphic development of tadpoles, which was arrested at stage X in all concentrations (Fig. 3). The inhibition of development in 155.67 mg/L PTU exposure was observed at day 7 of exposure, and in tadpoles exposed to 19.73 and 76.83 mg/L PTU became arrested at day 14 (Fig. 3). Moreover, tadpoles exposed to PTU exhibited a dose-dependent reduction in total body length (**Table 3**). The mortalities in each PTU exposure group were 0% (19.73 mg/L), 5% (76.83 mg/L), and 15% (155.67 mg/L) (**Table 2**). In the histological analysis, PTU-exposed tadpoles at 18 weeks after exposure were compared to control tadpoles that completed metamorphosis. In five tadpoles, the effects of PTU on thyroid gland were examined by histological analysis. Follicular hypertrophy and follicular cell hyperplasia were found in tadpoles exposed to 76.83 and 155.67 mg/L PTU. Thyroid gland hypertrophy was found in all PTU-exposed groups (Fig. 4). The effects of PTU were observed in all tadpoles, examined by histological analysis.

4. Discussion

The development of a test protocol using native amphibian species is important for assessment of ecological impacts of

Table 2
Mortalities of developing *R. rugosa* tadpoles in control, T_4, and PTU groups.

Groups	Replication no. of test tanks	Number of tadpoles	Mortality				
			Day 0	Day 7	Day 14	Day 21	Day 28
Control	3	30	0	0	0	1	1
T_4 (0.16 μg/L)	2	20	0	0	0	0	0
T_4 (0.61 μg/L)	2	20	0	0	0	0	1
T_4 (2.24 μg/L)	2	20	0	0	0	20	-
PTU (19.73 mg/L)	2	20	0	0	0	0	0
PTU (76.83 mg/L)	2	20	0	0	0	0	1
PTU (155.67 mg/L)	2	20	0	0	3	3	3

Table 3
Changes in total length (mm) of the developing tadpoles during exposure.

Chemicals	Mean (±SD)				
	Day 0	Day 7	Day 14	Day 21	Day 28
Control	20.40 (1.51)	25.42 (1.23)	31.48 (2.74)	37.02 (2.71)	42.59 (3.23)
T_4 (0.16 μg/L)	20.57 (1.44)	25.20 (2.04)	31.78 (2.76)	37.23 (3.55)	42.53 (4.11)
T_4 (0.61 μg/L)	19.69 (1.32)	24.63 (2.04)	30.54 (3.42)	34.18 (5.37)	34.48 (4.32)[a]
T_4 (2.24 μg/L)	20.79 (1.19)	24.29 (1.53)	24.47 (2.95)[a]	[b]	[b]
PTU (19.73 mg/L)	19.89 (1.25)	24.12 (2.41)	29.70 (3.10)	34.72 (4.07)	39.26 (4.80)[a]
PTU (76.83 mg/L)	20.34 (1.36)	24.22 (2.80)	28.55 (3.37)[a]	32.27 (3.88)[a]	35.81 (4.20)[a]
PTU (155.67 mg/L)	20.04 (1.11)	20.50 (2.46)[a]	23.02 (2.91)[a]	26.31 (2.60)[a]	28.69 (2.73)[a]

[a] $P<0.05$ vs. respective controls (Dunn's test).
[b] 11 tadpoles died or exhibited malformations.

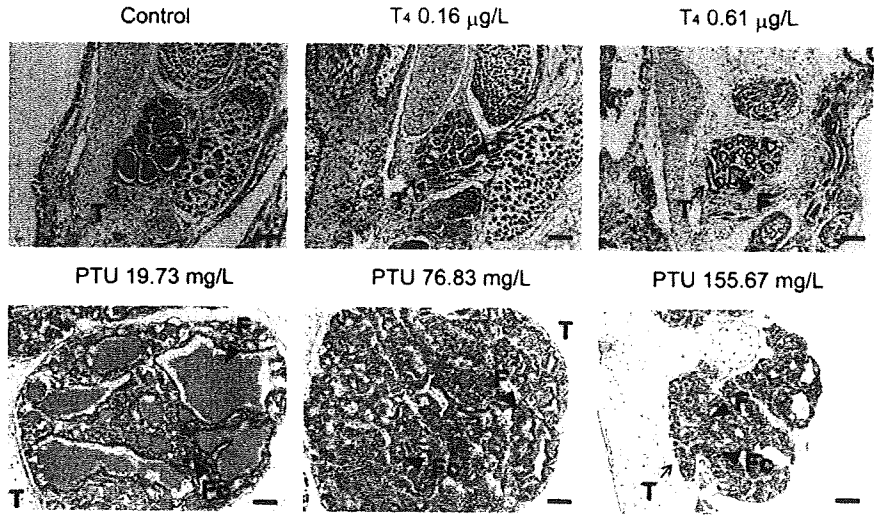

Fig. 4. Thyroid gland histology in *Rana rugosa* tadpoles at completed metamorphosis (T_4-exposed groups and controls) and tadpoles at 18 weeks after exposure (PTU-exposed groups). Five tadpoles in each group were used for histology. Control tadpole is shown in (A). Thyroid glands of 0.16 and 0.61 μg/L T_4-exposed tadpole are shown in (B) and (C), respectively. PTU (19.73, 76.83, and 155.67 mg/L)-exposed tadpoles are shown in (D), (E), and (F), respectively. T, thyroid gland; F, follicle; Fc, follicular cells, bar = 0.1 mm.

Table 4
Comparison of sensitivity of three anuran species to larval exposure to T_4 and PTU, as assessed by developmental stage (TK or NF) and total length.

Species	Temperature in each test (°C)	T_4 (Ac: 0.61 μg/L, Nc: 1 μg/L)		PTU (Ac: 76.83 μg/L, Nc: 75 μg/L)	
		Development (days[a])	Total length (days[a])	Development (days[a])	Total length (days[a])
Rana rugosa	25	14, 21, and 28	28	14, 21, and 28	14, 21, and 28
Xenopus laevis (**Opitz et al., 2005**)	25	7, 14, 21, and 28	14, 21, and 28	7, 14, 21, and 28	7, 14, 21, and 28
Xenopus tropicalis (**Mitsui et al., 2006**)	25	7, 14, 21, and 28	7, 14, 21, and 28	7, 14, 21, and 28	7, 14, 21, and 28

Ac: actual concentration; Nc: nominal concentration.
[a] The days showed statistical deference in the each endpoint.

chemicals. In the present study, *X. laevis* metamorphosis assay protocol was applied to *R. rugosa*, a native Japanese species for the first time, to establish the utility of this metamorphosis assay protocol for this species.

Initially we reared tadpoles at three different temperatures (22, 25, and 28 °C) to examine the effects of temperature on *R. rugosa* development and metamorphosis. In previous studies, *X. laevis* tadpoles typically reach a median stage of 56/57 in 28 days, starting from stage 49 (**Opitz et al., 2005**). Comparable developmental rate (a median stage of 56 in 28 days) was observed in our metamorphosis assay using *X. tropicalis* (**Mitsui et al., 2006**). In the present study, development was accelerated at 28 °C, while tadpoles reared at 25 °C developed at a similar rate to that of *X. laevis* and *X. tropicalis* on the basis of Taylor–Kollros/Nieuwkoop and Faber-stage comparisons (**Nieuwkoop and Faber, 1994**). Therefore, we selected 25 °C as the optimal temperature for the metamorphosis assay using *R. rugosa*.

R. rugosa tadpoles at developmental stages III/IV were exposed to T_4 and PTU for 28 days in semi-static conditions. In the chemical analysis of T_4, the recovery ratio of standard T_4 (0.2 μg/L) in methanol was 79.5%. In the test medium taken immediately after exposure, the actual T_4 concentrations were 50–60% of the nominal concentration in each exposure group. The samples at 2 days after exposure with the test medium containing tadpoles and feed were measured to determine the relative quantity of T_4 and PTU remaining, and the concentrations in each group decreased to less than 20% of the intended T_4.

T_4 (0.61 and 2.24 μg/L) and PTU (19.73, 76.83, and 155.67 mg/L) induced acceleration and inhibition of metamorphosis, respectively. These results were the same as those in *X. laevis* and *X. tropicalis* (**Degitz et al., 2005**; **Opitz et al., 2005**; **Mitsui et al., 2006**). The present results indicate that metamorphosis assay in *R. rugosa* can be used for detecting chemicals with agonistic and antagonistic activities of thyroid hormone, as has been shown in *X. laevis* and *X. tropicalis*. For screening of thyroid hormone-disrupting chemicals, histology of the thyroid gland was added as an endpoint in the test guideline of amphibian metamorphosis assay (**OECD, 2007**). In the present study, T_4 (0.16 and 0.61 μg/L)-exposed tadpoles, thyroid gland, and follicular sizes were smaller than those of controls. Follicular hypertrophy and follicular cell hyperplasia were found in tadpoles exposed to 76.83 and 155.67 mg/L PTU. Thyroid gland hypertrophy was found in all PTU groups. Since PTU-exposed groups showed no completed metamorphosis for 18 weeks after exposure, the histology of thyroid gland in PTU groups was compared to control tadpoles. In *X. laevis*, our unpublished data showed that 1 and 2 μg/L T_4 exposure showed thyroid gland atrophy in tadpoles at 21 days after exposure from stage 51. Moreover, **Degitz et al. (2005)** reported that PTU induced follicular hypertrophy at 5, 10, and 20 mg/L and follicular cell hyperplasia at 10 and 20 mg/L as results of the assay for 14 days from stage 51 in *X. laevis* tadpoles. Similar results were obtained in the present assay using *R. rugosa*.

In order to examine sensitivity to thyroid hormone agonist and antagonist, we compared the effects of T_4 and PTU on the

developmental stage during metamorphosis in three anuran species, *R. rugosa*, *X. laevis*, and *X. tropicalis* (Table 4). Since two previous studies using *X. laevis* (Opitz et al., 2005) and *X. tropicalis* (Mitsui et al., 2006) have been assessed in nominal concentrations, the present study using *R. rugosa* was compared using the nominal concentrations. In both *X. laevis* and *X. tropicalis* tadpoles, 1.0 μg/L T_4 and 75 mg/L PTU induced an acceleration and inhibition of metamorphic development, respectively, in comparison with the controls after a 7-day exposure. At the concentrations in the current test, T_4 (0.61 μg/L) and PTU (76.83 mg/L) accelerated and inhibited the metamorphosis of *R. rugosa* after 14-day exposure, respectively. As suggested by the present results, *R. rugosa* tadpoles showed slower responses to T_4 and PTU in comparison with *X. laevis* and *X. tropicalis*. However, this study demonstrates the successful application of an established anuran metamorphosis assay protocol to a native temperate Ranid species, *R. rugosa*, while further study using different chemicals will be needed to confirm the usefulness of this assay.

5. Conclusion

X. laevis metamorphosis assay (XEMA) protocol was applied to *R. rugosa*, a domestic species in Japan, for the first time to establish a detailed protocol of metamorphosis assay for this species. Moreover, we compared the effects of T_4 and PTU on metamorphosis of *R. rugosa* with published information for *X. laevis* and *X. tropicalis*. In the present study, *R. rugosa* can be used for detecting chemicals with agonistic and antagonistic activities of thyroid hormone, while *R. rugosa* tadpoles showed slower responses to T_4 and PTU in comparison with *X. laevis* and *X. tropicalis*. We demonstrated that the metamorphosis assay can be successfully applied to the domestic frog species.

Acknowledgments

We thank Dr. Daniel Pickford of Institute for the Environment, Brunel University, UK, for critical reading of this manuscript and Mr. Kenichi Masui of Environmental Chemistry Group, Idea Consultants, Inc., Shizuoka, Japan, for HPLC–MS analyses. This work was supported by grants from the Ministry of the Environment, Japan and the Ministry of Education, Culture, Sports, Science and Technology, Japan.

References

Amaya, E., Offield, M.F., Grainger, R.M., 1998. Frog genetics: *Xenopus tropicalis* jumps into the future. Trends Genet. 14, 253–255.

Colborn, T., vom Saal, F.S., Soto, A.M., 1993. Review. Developmental effects of endocrine-disrupting chemicals in wildlife and humans. Environ. Health Perspect. 101, 378–384.

Colborn, T., 1995. Environmental estrogens: health implications for humans and wildlife. Environ. Health Perspect. 103, 135–136.

Degitz, S.J., Holcombe, G.W., Flynn, K.M., Kosian, P.A., Korte, J.J., Tietge, J.E., 2005. Progress towards development of an amphibian-based thyroid screening assay using *Xenopus laevis*. Organismal and thyroidal responses to the model compounds 6-propylthiouracil, methimazole, and thyroxine. Toxicol. Sci. 87, 353–364.

Goleman, W.L., Urquidi, L.J., Anderson, T.A., Smith, E.E., Kendall, R.J., Carr, J.A., 2002. Environmentally relevant concentrations of ammonium perchlorate inhibit development and metamorphosis in *Xenopus laevis*. Environ. Toxicol. Chem. 21, 424–430.

Goto, Y., Kitamura, S., Kashiwagi, K., Oofusa, K., Tooi, O., Yoshizato, K., Sato, J., Ohta, S., Kashiwagi, A., 2006. Suppression of amphibian metamorphosis by bisphenol A and related chemical substances. J. Health Sci. 52, 160–168.

Gilchrist, M.J., Zorn, A.M., Voigt, J., Smith, J.C., Papalopulu, N., Amaya, E., 2004. Defining a large set of full-length clones from a *Xenopus tropicalis* EST project. Dev. Biol. 271, 498–516.

Grim, K.C., Wolfe, M., Braunbeck, T., Iguchi, T., Ohta, Y., Tooi, O., Touart, L., Douglas, C., Wolf, D.C., Tietge, J., 2009. Thyroid histopathology assessments for the amphibian metamorphosis assay to detect thyroid-active substances. Toxicol. Pathol., in press.

Hanada, H., Katsu, K., Kanno, T., Sato, E.F., Kashiwagi, A., Sasaki, J., Inoue, M., Utumi, K., 2003. Cyclosporin A inhibits thyroid hormone-induced shortening of the tadpole tail through membrane permeability transition. Comp. Biochem. Physiol. Part B 135, 473–483.

Hirsch, N., Zimmerman, L.B., Grainger, R.M., 2002. *Xenopus*, the next generation: *X. tropicalis* genetics and genomics. Dev. Dyn. 225, 422–433.

Kato, T., Matsui, K., Takase, M., Kobayashi, M., Nakamura, M., 2004. Expression of P450 aromatase protein in developing and in sex-reversed gonads of the XX/XY type of the frog *Rana rugosa*. Gen. Comp. Endocrinol. 137, 227–236.

Kitamura, S., Kato, T., Iida, M., Jinno, N., Suzuki, T., Ohta, S., Fujimoto, N., Hanada, H., Kashiwagi, K., Kashiwagi, A., 2005. Anti-thyroid hormonal activity of tetrabromobisphenol A, a flame retardant, and related compounds: affinity to the mammalian thyroid hormone receptor, and effect on tadpole metamorphosis. Life Sci. 76, 1589–1601.

Kloas, W., 2002. Amphibians as a model for the study of endocrine disruptors. Int. Rev. Cytol. 216, 1–57.

Kloas, W., Opitz, R., Lutz, I., 2003. Ringtest: effects of pesticides and other chemicals on thyroid system in the amphibian *Xenopus laevis*. Federal Environmental Agency Research Report 20067409, Berlin, Germany.

Nieuwkoop, P.D., Faber, J., 1994. Normal Table of *Xenopus laevis* (Daudin), third ed. Garland, New York.

Maeda, N., Matsui, M., 2003. Frogs and Toads of Japan, revised ed. Bun-ichi Sogo Shuppan Co., Ltd., Tokyo, Japan.

Mitsui, N., Fujii, T., Miyahara, M., Oka, T., Kashiwagi, A., Kashiwagi, K., Hanada, H., Urushitani, H., Santo, N., Tooi, O., Iguchi, T., 2006. Development of metamorphosis assay using *Silurana tropicalis* for the detection of thyroid system-disrupting chemicals. Ecotoxicol. Environ. Saf. 64, 281–287.

Miura, I., Ohtani, H., Kashiwagi, A., Hanada, H., Nakamura, M., 1996. Structural differences between XX and ZW sex lampbrush chromosomes in *Rana rugosa* females (Anura: Ranidae). Chromosoma 105, 237–241.

Miura, I., Ohtani, H., Hanada, H., Ichikawa, Y., Kashiwagi, A., Nakamura, M., 1997. Evidence for two successive pericentric inversions in sex lampbrush chromosomes of *Rana rugosa* (Anura: Ranidae). Chromosoma 106, 178–182.

Miura, I., Ohtani, H., Nakamura, M., Ichikawa, Y., Saitoh, K., 1998. The origin and differentiation of the heteromorphic sex chromosomes Z, W, X, and Y in the frog Rana rugosa, inferred from the sequences of a sex-linked gene, ADP/ATP translocase. Mol. Biol. Evol. 15, 1612–1619.

OECD, 2003. Second Meeting of the Validation Management Group for Ecotoxicity Tests (VMG-eco) of the Task Force on Endocrine Disrupters Testing and Assessment (EDTA), May 2, Organisation for Economic Co-operation and Development, Paris.

OECD, 2007. Guidance Document on Amphibian Thyroid Histology. In Environmental Health and Safety Publications, Series for Testing and Assessment, October 24, Organisation for Economic Co-operation and Development, Paris.

Opitz, R., Braunbeck, T., Bögi, C., Pickford, D.B., Nentwig, G., Oehlmann, J., Tooi, O., Lutz, I., Kloas, W., 2005. Description and initial evaluation of a *Xenopus* metamorphosis assay for detection of thyroid system-disrupting activities of environmental compounds. Environ. Toxicol. Chem. 24, 653–664.

Tata, J.R., 2006. Amphibian metamorphosis as a model for the developmental actions of thyroid hormone. Mol. Cell. Endocrinol. 246, 10–20.

Taylor, A.C., Kollros, J.J., 1946. Stages in the normal development of *Rana pipiens* larvae. Anat. Rec. 94, 7–23.

Tyler, C.R., Jobling, S., Sumpter, J.P., 1998. Endocrine disruption in wild life: a critical review of the evidence. Crit. Rev. Toxicol. 28, 319–361.

Development 136, 3969-3978 (2009) doi:10.1242/dev.039438

Dosage-dependent hedgehog signals integrated with Wnt/β-catenin signaling regulate external genitalia formation as an appendicular program

Shinichi Miyagawa[1,2], Anne Moon[3,*], Ryuma Haraguchi[2,*], Chie Inoue[4], Masayo Harada[1], Chiaki Nakahara[4], Kentaro Suzuki[1], Daisuke Matsumaru[4], Takehito Kaneko[2], Isao Matsuo[5], Lei Yang[6], Makoto M. Taketo[7], Taisen Iguchi[8], Sylvia M. Evans[9] and Gen Yamada[1,4,†]

Embryonic appendicular structures, such as the limb buds and the developing external genitalia, are suitable models with which to analyze the reciprocal interactions of growth factors in the regulation of outgrowth. Although several studies have evaluated the individual functions of different growth factors in appendicular growth, the coordinated function and integration of input from multiple signaling cascades is poorly understood. We demonstrate that a novel signaling cascade governs formation of the embryonic external genitalia [genital tubercle (GT)]. We show that the dosage of Shh signal is tightly associated with subsequent levels of Wnt/β-catenin activity and the extent of external genitalia outgrowth. In *Shh*-null mouse embryos, both expression of Wnt ligands and Wnt/β-catenin signaling activity are downregulated. β-catenin gain-of-function mutation rescues defective GT outgrowth and *Fgf8* expression in *Shh*-null embryos. These data indicate that Wnt/β-catenin signaling in the distal urethral epithelium acts downstream of Shh signaling during GT outgrowth. The current data also suggest that Wnt/β-catenin regulates *Fgf8* expression via Lef/Tcf binding sites in a 3′ conserved enhancer. Fgf8 induces phosphorylation of Erk1/2 and cell proliferation in the GT mesenchyme in vitro, yet *Fgf4/8* compound-mutant phenotypes indicate dispensable functions of *Fgf4/8* and the possibility of redundancy among multiple Fgfs in GT development. Our results provide new insights into the integration of growth factor signaling in the appendicular developmental programs that regulate external genitalia development.

KEY WORDS: External genitalia, Genetic cascade, Hedgehog, Fgf, β-catenin (Ctnnb1), Cloaca, Appendages, Mouse

INTRODUCTION

Embryonic development is controlled by a series of basic regulatory processes, including the regulation of protrusion and outgrowth. It has become clear that such developmental processes require coordinated reciprocal interactions between epithelium and the adjacent mesenchyme, frequently mediated through hedgehog, Wnt and fibroblast growth factor (Fgf) pathways. Perturbation of these pathways causes developmental abnormalities in a variety of tissues due, at least in part, to failed cross-talk. Despite the importance of this cross-talk and reciprocal interactions, our understanding of signaling pathway interactions is limited.

An embryonic bud structure (an appendage) is a representative organ that is suitable for analyzing reciprocal interactions between signaling pathways. Protruding embryonic buds are often composed of the distal epithelium accompanied by adjacent proliferating mesenchyme, which eventually gives rise to a bud structure. Significant progress has been achieved in understanding the molecular network that regulates limb development (Capdevila and Izpisua Belmonte, 2001; Chen et al., 2004; Johnson and Tabin, 1997; Kmita et al., 2005; Niswander, 2003; Yamaguchi et al., 1999; Yang et al., 2006; Zhu et al., 2008). Vertebrate limb development depends on the establishment and maintenance of the apical ectodermal ridge (AER), a specialized epithelium at the distal tip of the limb bud. Epithelial-mesenchymal interactions between the AER and its adjacent mesenchyme are essential for limb bud outgrowth. Fgf gene family members are expressed specifically in the AER. The cumulative evidence indicates that AER formation and maintenance and Fgf expression are tightly controlled by intricate interplay among several growth factors (Lewandoski et al., 2000; MacArthur et al., 1995; Mariani et al., 2008; Moon and Capecchi, 2000; Sun et al., 2000; Sun et al., 2002; Yu and Ornitz, 2008). Wnt/β-catenin signaling in the limb ectoderm regulates AER maintenance and *Fgf8* expression (Barrow et al., 2003; Soshnikova et al., 2003). Bmp signaling functions upstream of Wnt/β-catenin signaling in this process, as indicated by a failure of AER formation in mice lacking ectodermal bone morphogenetic protein receptor 1A (*Bmpr1a*) (Ahn et al., 2001). sonic hedgehog (*Shh*) is expressed in posterior limb bud mesenchyme [zone of polarizing activity (ZPA)] (Riddle et al., 1993), patterns the anterior-posterior axis of the limb, and supports expression of Fgf genes in the AER (Benazet et al., 2009; Laufer et al., 1994; Niswander et al., 1994; Riddle et al., 1993; Zuniga et al., 1999).

Another embryonic appendage, the genital tubercle (GT), is the common primordium of male and female external genitalia. GT outgrowth is the result of mesenchymal proliferation around the cloaca, accompanied by formation of the urethral plate epithelium at the ventral midline of the GT. The amniotic cavity and cloacal lumen are separated by two epithelial components: a superficial

[1]Institute of Molecular Embryology and Genetics, Global COE 'Cell Fate Regulation Research and Education Unit', and [2]Center for Animal Resources and Development, Kumamoto University, Kumamoto 860-0811, Japan. [3]Departments of Pediatrics, Neurobiology and Anatomy, and Human Genetics, University of Utah, UT 84112, USA. [4]Graduate School of Molecular and Genomic Pharmacy, Kumamoto University, Kumamoto 860-0811, Japan. [5]Osaka Medical Center and Research Institute for Maternal and Child Health, Osaka 594-1101, Japan. [6]Black Family Stem Cell Institute, Mount Sinai School of Medicine, New York, NY 10029, USA. [7]Graduate School of Medicine, Kyoto University, Kyoto 606-8501, Japan. [8]National Institutes of Natural Sciences, Okazaki 444-8787, Japan. [9]Skaggs School of Pharmacy, University of California, San Diego, CA 92093, USA.

*These authors contributed equally to this work
†Author for correspondence (gensan@gpo.kumamoto-u.ac.jp)

Accepted 14 October 2009

layer of ectodermal epithelium and a thick inner endodermal cell layer. A unique developmental property of the GT is the coordinated formation of endoderm-derived tissues during its outgrowth and patterning. The endodermal epithelium expresses *Shh*, which influences gene expression in the adjacent mesenchyme (Haraguchi et al., 2001; Perriton et al., 2002). *Shh*-deficient embryos exhibit GT agenesis with loss of *Bmp4* and *Fgf10* expression (Haraguchi et al., 2001; Perriton et al., 2002), suggesting that Shh functions high up in a signaling cascade governing GT development.

As appendages, limb buds and the GT exhibit similarities in their development; for example, they undergo prominent outgrowth as an embryonic bud structure before differentiation of tissue components (Cobb and Duboule, 2005; Dolle et al., 1991; Kondo et al., 1997; Yamada et al., 2003; Yamada et al., 2006). Given the accumulating evidence of the importance of Fgf signaling (and of Fgf8 in particular) from the AER, *Fgf8* is a prime candidate for mediating signaling from the GT epithelium to promote GT mesenchymal proliferation and outgrowth. The GT epithelium, termed the distal urethral epithelium (DUE), is located at the distal tip of the endoderm-derived epithelium (Haraguchi et al., 2001; Haraguchi et al., 2000; Lin et al., 2008; Ogino et al., 2001). Surgical removal of the tip of the GT, including the DUE, results in failure of GT outgrowth (Haraguchi et al., 2000). *Fgf8* has therefore been proposed as a candidate regulator of initial GT development, although its function in GT formation is unknown.

The prospective GT region of *Shh*-deficient embryos fails to express *Fgf8* (Haraguchi et al., 2001; Perriton et al., 2002), suggesting that *Fgf8* is genetically downstream of Shh signaling. Here we show that Wnt/β-catenin signaling plays a key role in GT formation by inducing multiple factors, including *Fgf8*. The temporal requirement of Shh function and the importance of hedgehog signaling dosage are shown by analysis of conditional *Shh* mutants and of a series of Gli mouse mutants. We demonstrate that Wnt/β-catenin pathway activation by Shh signaling is responsible for subsequent GT outgrowth, and postulate that Wnt/β-catenin signaling functions in the DUE to stimulate mitogenic factors for the adjacent mesenchyme. Altogether, these data suggest a similar, and yet divergent, participation of growth factor signaling pathways, including Shh, Wnt/β-catenin and Fgf, in the development of appendicular structure, the external genitalia.

MATERIALS AND METHODS

Mouse strains and embryos

The mutant mice used were *Shh* (Chiang et al., 1996), *Gli2* (Mo et al., 1997), $Gli3^{xt}$ (Hui and Joyner, 1993), $Shh^{CreERT2}$ (Harfe et al., 2004), $Isl1^{Cre}$ (Yang et al., 2006), *Hoxa3-Cre* (Macatee et al., 2003), β-catenin^{Ex3} ($Ctnnb1^{Ex3}$) (Harada et al., 1999), β-catenin^{lox} ($Ctnnb1^{lox}$) (Huelsken et al., 2001), Shh^{lox} (Dassule et al., 2000), $Fgf4^{lox}$ (Moon et al., 2000), $Fgf8^{lox}$ (Park et al., 2006), *R26R* (Soriano, 1999), *TopGAL* (DasGupta and Fuchs, 1999) and *BatGAL* (Nakaya et al., 2005). To increase the efficiency of production of homozygous null embryos and decrease the incidence of mosaic deletion, β-catenin-null alleles were generated by utilizing *CAGGS-Cre* mice (Araki et al., 1997), which express Cre recombinase in the germline. Noon on the day when a vaginal plug was detected was designated as E0.5. Embryos for each experiment were collected from at least three pregnant females. All procedures and protocols were approved by the Committee on Animal Research at Kumamoto University, Japan.

The tamoxifen (TM)-inducible Cre recombinase system removes the floxed sequence from the target genome (Feil et al., 1997). TM (Sigma, St Louis, MO, USA) was dissolved in sesame oil at 10 mg/ml. Four milligrams ($Ctnnb1^{lox}$ mice) or 2 mg ($Ctnnb1^{Ex3}$ and Shh^{lox} mice) of TM per 40 g body weight was used to treat the pregnant mice. Under these conditions, no overt teratologic effects on the urogenital organs are observed (Haraguchi et al., 2007).

Histology

Hematoxylin and Eosin staining, X-Gal staining, immunohistochemistry and in situ hybridization for gene expression were performed by standard procedures as previously described (Haraguchi et al., 2007). Immunohistochemistry employed the following primary antibodies: Cd44, β-catenin, E-cadherin (BD Biosciences, Franklin Lakes, NJ, USA) and phospho-Erk1/2 (Cell Signaling, Danvers, MA, USA). For in situ hybridization, the following riboprobe templates were used: *Tcf1* (H. Clevers, University Medical Center Utrecht, The Netherlands); *Pitx1* (Y. Chen, Tulane University, New Orleans, LA, USA); *Fgf3* (C. Dickson, Imperial Cancer Research Fund, London, UK); *Fgf4* (G. Martin, University of California, San Francisco, CA, USA); *Wnt3*, *Wnt4*, *Wnt5a*, *Wnt7a*, *Wnt9b* (S. Takada, National Institutes of Natural Sciences, Okazaki, Japan); and *Fgf4*, *Fgf8*, *Fgf10*, *Bmp4*, *Gli1*, *Ptch1*, *Shh*, *Dlx5* (Haraguchi et al., 2007; Suzuki et al., 2008). The template of *Axin2* was obtained by standard RT-PCR procedures using primers 5′-CCACTTCAAGGAGCAGCTCAGCA-3′ and 5′-TACCCAGGCTCCTGGAGACTGA-3′.

Cell proliferation and death analyses

Pregnant females were injected with 100 mg BrdU (Sigma) per kg body weight. One hour after injection, embryos were collected. For cell culture experiments, BrdU (1 μg/ml) was added to the medium for 30 minutes and BrdU incorporation detected with anti-BrdU antibody (Roche, Mannheim, Germany). TUNEL assay for the detection of apoptotic cells was performed with the In Situ Apoptosis Detection Kit (Takara, Ohtsu, Japan).

Organ culture

Filter-supported organ cultures for murine GTs isolated from embryos of ICR strain (E11.5; CLEA, Tokyo, Japan) were as previously described (Haraguchi et al., 2000). The tissues were cultured for 24 hours after bead application and processed for histological analysis. Heparin acrylic beads were soaked overnight with recombinant mouse Fgf8b protein at 1.0 mg/ml in PBS (Haraguchi et al., 2000). Control beads were treated with PBS containing 0.1% BSA.

Plasmid DNA and luciferase assay

The conserved region 3′ of the *Fgf8* locus was described previously (Beermann et al., 2006). Genomic sequences of the 5′ region and conserved region 3 (CR3) of *Fgf8* loci, obtained from Ensemble (www.ensembl.org), were submitted for analysis by rVISTA (genome.lbl.gov/vista). DNA fragments of CR3 of the murine *Fgf8* locus, obtained from a BAC clone (RPCI23-98F2) by PCR, were inserted into the pGL4.24 vector (Promega, Madison, WI, USA). The mouse β-catenin expression vector was kindly provided by Dr S. Kume (Takahashi et al., 2000).

The HaCat cell line was maintained in DMEM supplemented with 10% FBS. Cells were transfected with expression and reporter plasmids using FuGENE HD (Roche) according to the manufacturer's instruction. Twenty-four to thirty hours post-transfection, luciferase activity was measured by chemiluminescence employing the Dual-Luciferase Reporter Assay System (Promega). The values were normalized against *Renilla* luciferase activity. At least three independent experiments were performed. Statistical analysis was performed using Student's *t*-test or Welch's *t*-test followed by F-test ($P<0.05$ considered significant).

Chromatin immunoprecipitation (ChIP) assay

The ChIP Assay Kit (Upstate, Lake Placid, NY, USA) was used. The distal GT region containing the DUE, and the distal tip of the hindlimb containing the AER, were dissected from embryos at E12.5 and E10.5, respectively. β-catenin (Santa Cruz) and acetyl-histone H3 (Upstate) antibodies (2 μg) were used. For mock control, rabbit or mouse immunoglobulin (Dako, Carpinteria, CA, USA) was used. More than three independent experiments were performed. PCR was performed with the following primers: 5′ flanking region, 5′-CAGAGAGAGCCGTTTGTGTTGG-3′ and 5′-TCAAAGCCCCGTAATTACAATTGC-3′; CR3, 5′-CTGGCTGAAA-GCCACAGACG-3′ and 5′-GCTGGGTCTCTGCTGGTAACC-3′.

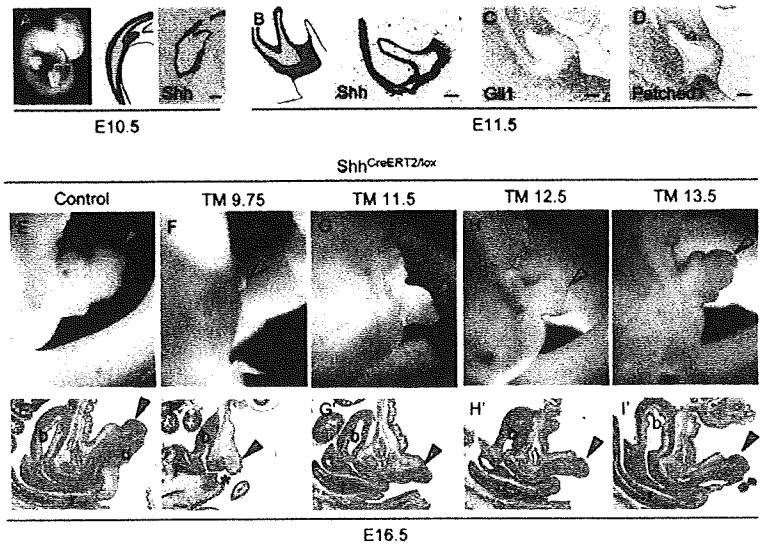

Fig. 1. Temporal requirements for hedgehog signaling during GT initiation and outgrowth. (**A,B**) Murine GT development and *Shh* expression at E10.5 (A) and E11.5 (B). Red regions indicate *Shh*-expressing endoderm-derived epithelia. The cloacal region includes the thick endodermal epithelia (in red, B). The dark-blue line indicates adjacent ectoderm-derived epithelium. Cloacal cavity is in light blue. (**C,D**) *Gli1* (C) and patched 1 (D) expression in GT mesenchyme and ectoderm at E11.5. (**E-I'**) Phenotypes after temporally staggered ablation of *Shh*. GT phenotypes of $Shh^{CreERT2/lox}$ embryos treated with TM at E9.75 (F), E11.5 (G), E12.5 (H) and E13.5 (I) versus the control GT (no TM administration, E). TM administration at E9.75 induced severe GT aplasia with a persistent cloaca (asterisk). Arrowheads indicate GTs or GT rudiments. b, bladder; r, rectum; u, urethra. Scale bars: 100 μm.

RESULTS

Progressive GT formation revealed by conditional *Shh* mutation

The murine GT begins to visibly protrude as a bud structure at E10.5-11.5. *Shh* is expressed in the endodermal cloacal epithelium at this time (Fig. 1A,B) and the hedgehog-responsive genes *Gli1* and patched 1 (*Ptch1*) are expressed in the adjacent mesenchyme and ectoderm (Fig. 1C,D). *Shh* knockout (KO; *Shh*) embryos exhibit a complete failure of GT outgrowth (Haraguchi et al., 2001). We analyzed the temporal dependence of GT development on Shh genetically by crossing $Shh^{CreERT2}$ and Shh^{lox} alleles, which permits inducible Cre function and *Shh* inactivation in the cloacal endodermal cells and in cells of urethral plate epithelium (UPE) upon TM administration (Harfe et al., 2004). In control embryos, a prominent GT protrusion was observed, the bladder developed normally, and the urethral and rectal orifices were completely separated (Fig. 1E). In $Shh^{CreERT2/lox}$ mutants, administration of TM at E9.75 caused severe GT hypoplasia, accompanied by a persistent cloaca; the urethral and rectal ends were shared and opened at a common orifice in the rudimentary GT (Fig. 1F). Expression of the distal marker genes *Wnt5a* and *Dlx5* was not detected in the mutants, although expression of *Pitx1* as a dorsal marker was still observed (see Fig. S1 in the supplementary material). TM administration at sequentially later stages elicited progressively milder GT phenotypes (Fig. 1G-I), such that administration of TM at E13.5 resulted in morphologically normal GTs.

Decreased expression of Wnt ligand genes in *Shh* mutant GT

Shh elicits mesenchymal and epithelial cellular responses and regulates the expression of several downstream genes during GT development (Haraguchi et al., 2001). However, the signaling pathways downstream of Shh that are required for GT development have not been identified. Because of the importance of Fgf/Shh interactions in limb AER and mesenchyme, and given that Wnt ligands can regulate *Fgf8* expression and limb outgrowth (Barrow et al., 2003; Kawakami et al., 2001; Kengaku et al., 1998), we examined the expression of Wnt ligand genes in the GT. Several Wnt ligand genes were expressed in the GT (as assessed by RT-PCR, data not shown). Among them, *Wnt3*, *Wnt4*, *Wnt7a* and *Wnt9b* were downregulated in the GT of *Shh* KO mutant embryos (Fig. 2A-D), particularly in the GT ectoderm (Fig. 2E-H).

Regulation of Wnt/β-catenin activity by Shh signaling

To examine whether the decreased expression of ectodermal Wnt ligands results in decreased Wnt/β-catenin signaling in *Shh* KO mutants, we assayed β-galactosidase (β-gal) activity from the *TopGAL* allele (DasGupta and Fuchs, 1999). During normal GT development, weak β-gal activity is detected in the cloacal region at E10.5 (Fig. 3A) (Lin et al., 2008). At E11.5, increased β-gal activity was observed in the distal region of the endodermal epithelium (Fig. 3B-D), which overlapped, in part, with the DUE as defined by *Fgf8*

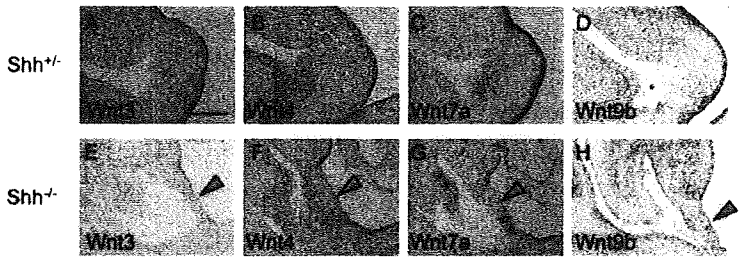

Fig. 2. Expression of Wnt ligands in control and *Shh* KO mouse embryos at E11.5. (**A-H**) Ectodermal expression (arrowheads) of *Wnt3* (A,E), *Wnt4* (B,F), *Wnt7a* (C,G) and *Wnt9b* (D,H) is decreased in *Shh* KO embryos. Scale bar: 100 μm.

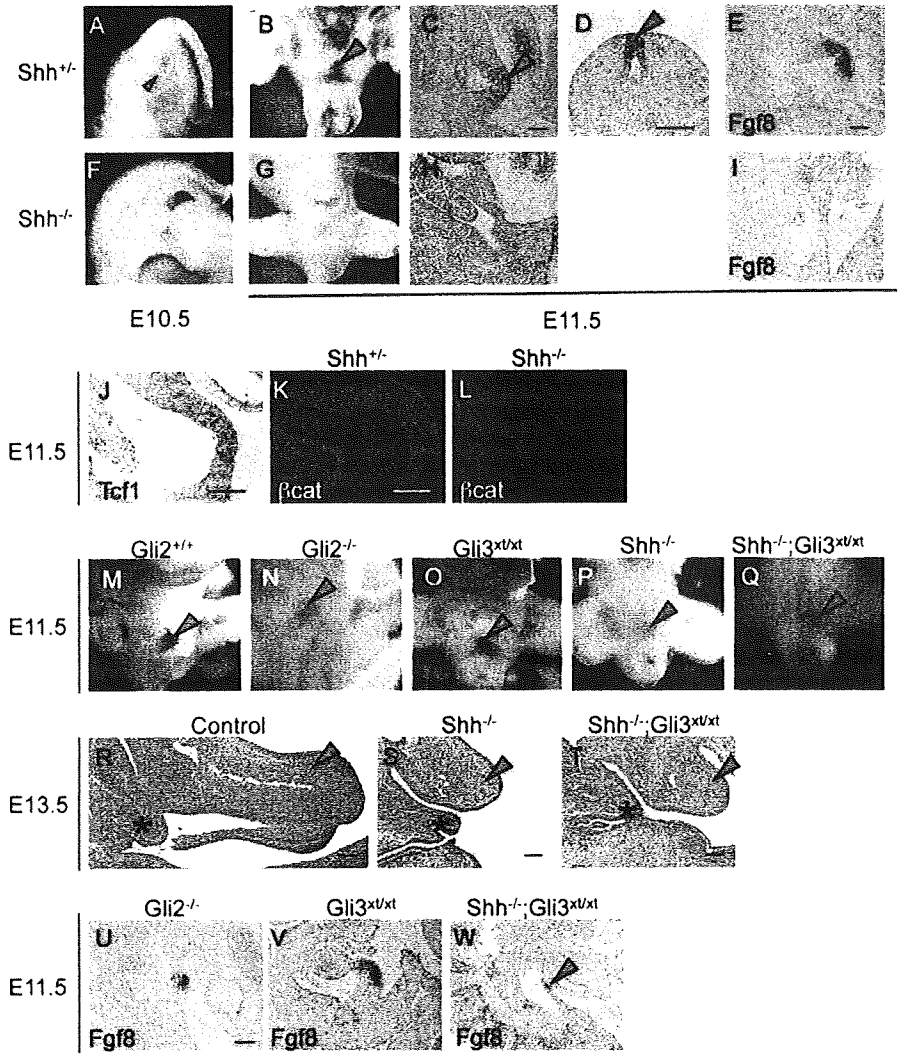

Fig. 3. Wnt/β-catenin signaling is responsive to hedgehog signaling dosage in the mouse GT. (**A-E**) TopGAL activity (arrowheads) is detectable in the distal region of the GT, including the DUE at E10.5 (A) and E11.5 (B-D). *lacZ* staining (C,D, arrowheads) overlaps with the *Fgf8* expression domain (E). (**F-I**) TopGAL activity (F-H) and *Fgf8* expression (I) are not detected in *Shh* KO embryos. (**J**) *Tcf1* is expressed in the distal GT. (**K,L**) β-catenin protein localizes predominantly to the endodermal epithelium (K, green) and decreases in *Shh* KO embryos (L). (**M-Q**) *Gli2* KO embryos have decreased TopGAL reporter activity (N) relative to control (M) and $Gli3^{xt/xt}$ embryos (O). $Shh^{-/-};Gli3^{xt/xt}$ double mutants exhibit weak, but detectable, TopGAL activity (Q, arrowhead) as compared with *Shh* KO embryos (P). (**R-T**) Sections of control (R), *Shh* KO (S) and $Shh^{-/-};Gli3^{xt/xt}$ (T) embryos. GT outgrowth is restored in the $Shh^{-/-};Gli3^{xt/xt}$ double mutants at E13.5 (arrowhead). Asterisk indicates the distal end of the urorectal septum. (**U-W**) GT outgrowth and *Fgf8* expression in hedgehog pathway mutants at E11.5. Decreased *Fgf8* expression and GT hypoplasia in *Gli2* KO embryos (U, compare with E). $Gli3^{xt/xt}$ embryos have normal GT protrusion and *Fgf8* expression (V). $Shh^{-/-};Gli3^{xt/xt}$ embryos exhibit a small bud structure with some *Fgf8* expression (W, arrowhead). Scale bars: 100 μm.

expression (Fig. 3E). This β-gal activity in the DUE persisted throughout multiple stages of GT development (see Fig. S2 in the supplementary material). In *Shh* KO embryos, TopGAL activity was almost undetectable in the cloaca at E10.5 and E11.5 (Fig. 3F-H), and was accompanied by a loss of *Fgf8* expression in the DUE (Fig. 3I). We obtained similar results with the *BatGAL* allele (see Fig. S3 in the supplementary material), another Wnt/β-catenin signaling indicator mouse line (Nakaya et al., 2005). β-catenin (*Ctnnb1*) and *Tcf1* (*Tcf7* – Mouse Genome Informatics) encode essential components of the Wnt signaling pathway and are expressed in the cloacal epithelium in an overlapping manner (Fig. 3J,K). β-catenin immunoreactivity in the cloacal epithelium and in the distal endodermal epithelium (inclusive of the DUE) was reduced in *Shh* KO embryos relative to controls at E11.5 (Fig. 3L). In $Shh^{CreERT2/lox}$ mutants, E-cadherin (cadherin 1) expression in the cloacal membrane was normal, whereas β-catenin expression was decreased (see Fig. S4 in the supplementary material). These results suggest that decreased Wnt activity in the *Shh* mutants is likely to be induced by the defective signaling cascade.

We then assessed TopGAL activity in mouse mutants of various hedgehog signaling components. In *Gli2* KO embryos, β-gal activity was decreased and the GT hypoplasic, consistent with the general role of Gli2 as a positive effector of Shh signaling (Fig. 3M,N). Gli3 generally functions as a transcriptional repressor for hedgehog signaling (Ingham and McMahon, 2001). Although *Gli3* mutants ($Gli3^{xt/xt}$) do not have significant defects in GT outgrowth, *Shh;Gli3* double-mutant embryos ($Shh^{-/-};Gli3^{xt/xt}$) restored TopGAL activity in the GT relative to that in *Shh* mutants, consistent with the dosage sensitivity of this structure to *Shh* (Fig. 3O-Q). GT outgrowth was detectable at E13.5 in *Shh;Gli3* double mutants, indicating partial rescue of the effect of *Shh* loss-of-function on outgrowth (Fig. 3R-T). These results are the first demonstration of the integrated effects of Gli2 and Gli3 in mediating hedgehog-dependent GT development, and of the dependence of Wnt/β-catenin activity during GT formation on Shh signaling. The activity of both signaling pathways correlates with the extent of GT outgrowth and *Fgf8* expression (Fig. 3U-W).

Requirement for β-catenin during GT development

Wnt/β-catenin signaling is required for caudal body formation; $Wnt3a^{-/-}$, $Lef1^{-/-};Tcf1^{-/-}$ and $Tcf1^{-/-};Tcf4^{-/-}$ embryos exhibit severe caudal truncation with GT agenesis (Dunty et al., 2008; Galceran et al., 1999; Gregorieff et al., 2004; Takada et al., 1994). To focus on the role of β-catenin specifically during GT formation, β-catenin

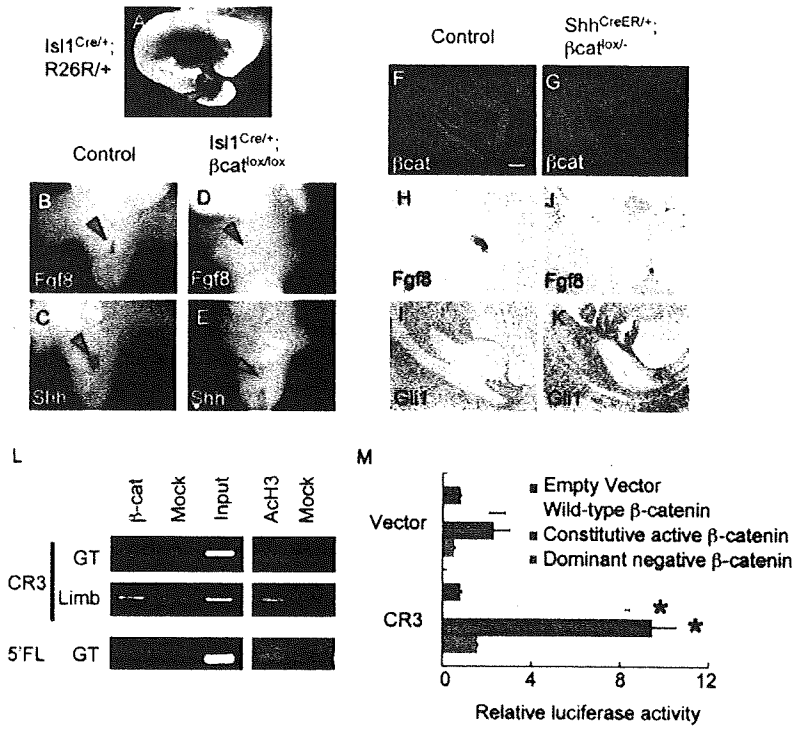

Fig. 4. Gene expression in β-catenin loss-of-function mutants. (**A**) *Isl1-Cre*-mediated *lacZ* expression in *R26R* mice. Cre is active in the caudal E9.0 embryo (arrowhead). (**B-E**) E11.5 control embryos (B,C). *Fgf8* (D) and *Shh* (E) expression (arrowheads) in $Isl^{Cre/+}$;$Ctnnb1^{lox/lox}$ embryos. (**F-K**) Failed GT outgrowth in E11.5 endoderm-specific β-catenin (βcat) conditional mutants (F,G). Green, immunofluorescence for β-catenin; blue, Hoechst counterstain. *Fgf8* expression is abnormal (H,J), whereas *Gli1* is normal (I,K), at E11.5. (**L**) ChIP/PCR on GT and limb reveals that β-catenin can bind to the murine CR3 region but not to the 5′ flanking region. Acetylated histone H3 is bound to both regions. (**M**) The CR3 putative enhancer activates expression of a luciferase reporter in response to overexpressed wild-type or constitutively active β-catenin. *, $P<0.05$ versus empty vector control. Scale bar: 100 μm.

conditional mutant mice were analyzed. We employed the $Isl1^{Cre}$ line as it drives Cre activity in the caudal region of embryos as early as E9.0 (Fig. 4A). Thus, $Isl1^{Cre}$ is useful for analyzing the developmental processes in the prospective GT region before GT outgrowth. In $Isl1^{Cre/-}$;$Ctnnb1^{lox/lox}$ mutants, the GT failed to protrude and expression of *Fgf8* and *Shh* was absent in the DUE at E11.5 (Fig. 4B-E). This raises the intriguing possibility that an early phase of β-catenin activity is necessary for cloacal *Shh* expression.

By contrast, the temporally inducible $Shh^{CreERT2}$ line is suitable for analyzing gene function during later stages of GT development, as Shh-dependent outgrowth proceeds. In $Shh^{CreERT2/-}$;$Ctnnb1^{lox/-}$ embryos, the levels of β-catenin protein in the GT region (including the DUE) were reduced at E11.5 and GT outgrowth failed (Fig. 4F,G). *Fgf8* expression was markedly reduced in the mutants (Fig. 4H,J). *Gli1* was expressed normally at these stages (Fig. 4I,K), indicating that Shh signaling is not dependent on Wnt/β-catenin signaling at this later stage.

Potential regulation of *Fgf8* expression by β-catenin

To examine the possibility that *Fgf8* expression is directly regulated by β-catenin, chromatin immunoprecipitation (ChIP) and reporter assays were performed for a region 3′ of the *Fgf8* locus that contains an evolutionarily highly conserved putative *Fgf8* enhancer. Conserved region 3 [CR3 (Beermann et al., 2006)] is a candidate enhancer that regulates reporter expression in the AER, and we considered whether it might also function as a DUE enhancer given the similarities between the DUE and the AER as a transient distal signaling epithelium. Using rVISTA, we found that CR3 contains several Lef/Tcf binding sites (see Fig. S5 in the supplementary material). We performed a ChIP assay followed by PCR using primers that amplify a CR3 genomic fragment that includes these binding sites. β-catenin-specific enrichment was observed in the extracts from the GT and limb bud (Fig. 4L). PCR amplification of a putative enhancer 5′ of *Fgf8* (Hu et al., 2004), which is also highly conserved in vertebrates but lacks Lef/Tcf binding sites, yielded no enrichment (Fig. 4L). Both regions were enriched in chromatin immunoprecipitated with anti-acetylated histone H3, as a positive control. Furthermore, overexpression of wild-type or constitutively active β-catenin activated transcription of a CR3 enhancer/luciferase reporter in HaCat cells, whereas a dominant-negative form did not (Fig. 4M). Taken together, these results suggest that Wnt/β-catenin signaling participates in the regulation of *Fgf8* expression via CR3.

Fgf8 can induce phosphorylation of Erk1/2 and cell proliferation in GT mesenchyme, but Fgf4 and Fgf8 are dispensable for GT outgrowth

In the limb, AER-derived Fgf induces phosphorylated (p) Erk1/2 (Mapk3/1 – Mouse Genome informatics) activity in the adjacent mesenchyme (Kawakami et al., 2003). Organ culture experiments with explanted GTs revealed that GT mesenchyme adjacent to Fgf8b-soaked beads has a higher level of pErk1/2 than that with a contralaterally implanted control bead (Fig. 5A). GT mesenchymal cell proliferation was also consistently increased by Fgf8b treatment of cultured GTs (Fig. 5B).

To investigate Fgf functions during GT development in vivo, we conditionally inactivated *Fgf8* in the GT with a *Hoxa3-Cre* line, which exhibits strong Cre activity throughout the caudal embryo, including the presumptive cloacal region, GT primordium and DUE (see Fig. S6A in the supplementary material) (Macatee et al., 2003). In situ hybridization using an *Fgf8* antisense riboprobe specific for the floxed exon 5 (Moon and Capecchi, 2000) confirmed the absence of *Fgf8* expression in the *Hoxa3-Cre;Fgf8* mutants (see Fig. S6B,C in the supplementary material). Notably, we found that although *Fgf4* expression was barely detected in the normal GT, ablation of *Fgf8* resulted in increased *Fgf4* expression in the DUE

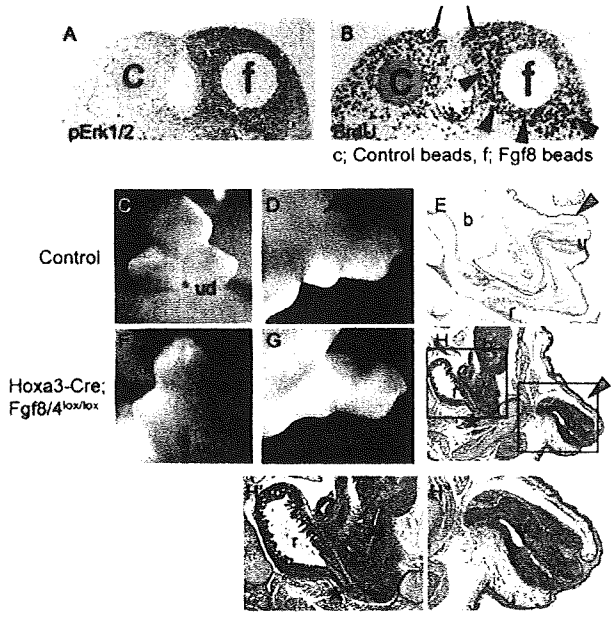

Fig. 5. *Fgf8* and *Fgf4* are dispensable for mouse GT development. (**A**,**B**) Anti-pErk1/2 and BrdU immunostaining in GT explants. pErk1/2 activity is restricted to distal GT with the control (c) bead (A). pErk1/2 (A) and BrdU incorporation (B) are augmented in regions adjacent to Fgf8 (f) beads. Arrowheads and arrows indicate augmented and endogenous cell proliferation, respectively. (**C-H″**) GT phenotype of control (C-E) and *Hoxa3-Cre;Fgf8/4*$^{lox/lox}$ mutant embryos (F-H″) at E14.5 (C,D,F,G) and E18.5 (E,H-H″). GT outgrowth appears normal in mutants (arrowheads), but the urogenital duct (ud) is wide open and anal stenosis (asterisk) and urethral narrowing with proximal atresia are also present. The distal urethra appears normal. b, bladder; r, rectum; u, urethra.

(see Fig. S6D,E in the supplementary material), similar to what has been reported following *Fgf8* ablation in the AER (Lewandoski et al., 2000; Moon and Capecchi, 2000). We analyzed *Fgf8;Fgf4* double-mutant embryos and found, surprisingly, that the mutant GT appeared to have normal outgrowth at E14.5 (Fig. 5C,D,F,G) and only mild abnormalities of the external genitalia at E18.5. However, these mutants did have anal stenosis and a narrowed, proximally atretic urethra, whereas the distal urethra appeared normal (Fig. 5E,H). Thus, although Fgf8 can induce Erk1/2 phosphorylation and cell proliferation in the GT in vitro, it is dispensable for GT outgrowth. In the AER and elsewhere, Fgf ligands have overlapping expression patterns and functional redundancy has been reported (Boulet et al., 2004; Ladher et al., 2005; Mariani et al., 2008; Moon and Capecchi, 2000; Sun et al., 2002). In addition to *Fgf4*, we also found increased expression of *Fgf3* in the distal GT and in the limb of *Hoxa3-Cre;Fgf8*$^{lox/lox}$*;Fgf4*$^{lox/lox}$ (*Fgf8/4*$^{lox/lox}$) mutants (see Fig. S7 in the supplementary material).

Constitutively active β-catenin rescues GT outgrowth in *Shh* mutants

Our current findings suggest that β-catenin functions downstream of Shh to support GT outgrowth; if so, overexpression of β-catenin should at least partially rescue GT agenesis in *Shh* KO mutants. We generated *Shh*$^{CreERT2/-}$*;Ctnnb1*$^{Ex3/-}$ mutant embryos, which express a constitutively active β-catenin (*Ctnnb1*^{Ex3}) in a *Shh*-null background. Indeed, TM treatment at E9.5 resulted in visible outgrowth of the GTs of these compound mutants at E11.5, in contrast to GT agenesis in the *Shh*$^{CreERT2/-}$*;Ctnnb1*$^{+/+}$ (equivalent to the *Shh*-null) embryos (Fig. 6A-C). At E13.5, GT outgrowth and a preputial fold were present, although smaller than normal (Fig. 6F-H). Surviving mutant embryos at E18.5 displayed a bud structure composed of mesenchymal tissue without the urethra (Fig. 6I,J; data not shown). It is noteworthy that hedgehog signaling was not activated in the *Shh*$^{CreERT2/-}$*; Ctnnb1*$^{Ex3/+}$ embryos, judging by *Gli1* expression (Fig. 6D,E), whereas *Fgf8* was expressed at high level in the *Shh*$^{CreERT2/-}$*;Ctnnb1*$^{Ex3/+}$ embryos (Fig. 7A-C). The *Fgf8* expression domain coincided with the location of β-catenin augmentation, as evident by expression of *Axin2*, a downstream target of the Wnt/β-catenin pathway (Fig. 7D-F).

Cd44, another AER marker (Sherman et al., 1998), is expressed in a similar manner to *Fgf8* in the DUE (Fig. 7G). Consistent with rescued *Fgf8* expression in *Shh*$^{CreERT2/-}$*;Ctnnb1*$^{Ex3/-}$ embryos, Cd44 expression was also restored (Fig. 7H,I). Expression of *Fgf10* and *Bmp4* in the GT mesenchyme is regulated by *Shh* and, consequently, their expression is decreased in *Shh* KO embryos (see Fig. S8A,B,D,E in the supplementary material) (Haraguchi et al., 2001; Perriton et al., 2002). *Fgf10* and *Bmp4* expression was not rescued in the GT mesenchyme of *Shh*$^{CreERT2/-}$*;Ctnnb1*$^{Ex3/-}$ embryos (see Fig. S8C,F in the supplementary material).

In wild-type mouse embryos, pErk1/2 immunoreactivity is present mainly in the mesenchyme (Fig. 7J), and is decreased in *Shh* KO embryos (Fig. 7K). By contrast, the mesenchymal domain of pErk1/2 expression was markedly enhanced in the GT of *Shh*$^{CreERT2/-}$*;Ctnnb1*$^{Ex3/-}$ embryos (Fig. 7L), consistent with increased Fgf8 signaling. Abundant cell proliferation was observed in control embryos (Fig. 7M), but in *Shh* KO embryos mesenchymal cell proliferation was specifically decreased (Fig. 7N). Cell death in the endodermal epithelium and mesenchyme was increased in the distal GT (Fig. 7P,Q). It has been reported that the normal DUE, as with other signaling epithelia, displays a scattered pattern of apoptosis concomitant with reduced cell proliferation (Fig. 7M,P) (Haraguchi et al., 2001; Jernvall et al., 1998). In *Shh*$^{CreERT2/-}$*;Ctnnb1*$^{Ex3/-}$ embryos, mesenchymal cell proliferation was largely rescued (Fig. 7O), but mesenchymal cell death remained elevated above that seen in controls (Fig. 7R).

DISCUSSION

Coordinated growth factor signaling is essential for regulating morphogenesis of appendicular structures such as the limbs and external genitalia. Although previous studies significantly advanced our knowledge of individual gene contributions, understanding how these genes interact and how multiple signaling inputs are integrated during organogenesis remains a major challenge. Here we report that hedgehog signaling is essential for external genitalia development in a dosage-dependent manner, as demonstrated by analyses of different Gli compound mutants. Different levels of hedgehog signaling modulate the level of Wnt/β-catenin activity to regulate outgrowth of the embryonic external genitalia. *Shh* KO embryos display a persistent cloaca and failed GT outgrowth (Haraguchi et al., 2001; Mo et al., 2001; Perriton et al., 2002). Remarkably, we found that overexpression of constitutively active β-catenin rescues GT protrusion in the absence of *Shh* and *Fgf8* expression in the endoderm is restored as is mesenchymal proliferation. To our knowledge, this is the first demonstration of genetic rescue of embryonic appendicular agenesis.